Progress In Electromagnetics Research, Vol. 116, 475–515, 2011

APPLICATION OF THE NEWTON METHOD TO IMPROVE THE ACCURACY OF TOA ESTIMATION WITH THE BEAMFORMING ALGORITHM AND THE MUSIC ALGORITHM

J.-H. Lee

Department of Information and Communication Engineering
Sejong University, Seoul 143-747, Korea

Y. S. Jeong

Radar System Group, System 1 Team, R & D Center,
Samsung Thales Co., Ltd., Gyeonggi-Do 446-712, Korea

S.-W. Cho and W.-Y. Yeo

Department of Information and Communication Engineering
Sejong University, Seoul 143-747, Korea

K. Pister

Department of Electrical Engineering and Computer Science
UC Berkeley, Berkeley, CA 94720, USA

Abstract—In this paper, a numerical method for improving the performance of the beamforming algorithm and the MUSIC algorithm for TOA (Time-of-arrival) estimation is presented. It has been shown that the conventional beamforming algorithm and the MUSIC algorithm can be used for time delay estimation. Using the beamforming algorithm and the MUSIC algorithm for TOA estimation, the initial estimate for the TOA is obtained. To improve the accuracy of the TOA estimation, we apply the Newton iteration to the initial estimate. The initial estimates obtained from the beamforming algorithm and the MUSIC algorithm are updated to obtain the final estimates which are more accurate than the initial estimates in terms of the RMSE (Root Mean Square Error). To find the TOA which maximizes the beamforming spectrum or the MUSIC spectrum, we find

Received 26 November 2010, Accepted 4 May 2011, Scheduled 17 May 2011
Corresponding author: Joon-Ho Lee (joonhlee@sejong.ac.kr).

the TOA at which the derivative of the beamforming spectrum with respect to the delay is zero. To find numerically the TOA at which the derivative of the beamforming spectrum or the MUSIC spectrum is zero, the Newton iteration is adopted. In numerical results, the validity of the proposed scheme is illustrated using various examples.

1. INTRODUCTION

Determination of the TOA (time-of-arrival) [1–9, 33] of a incident signal has been of interest to the signal processing community. The estimation of the TOA has many applications which range from military to civilian applications. The main application of DOA and AOA estimation is the wireless localization. There has been much research on wireless localization [13–24].

What is the most important in the TOA estimation is how to achieve good estimation accuracy. In this paper, we propose how to improve the accuracy of the TOA estimation using numerical method. The scheme is based on the Newton iteration applied to the cost function derived from the TOA estimation. Using the initial estimate obtained from the time delay estimation, the initial estimate is updated iteratively using the Newton iteration. The final estimate obtained after the iterative refinement is more accurate than the initial estimate.

In this paper, we use the conventional beamforming algorithm and the MUSIC algorithm to get the initial estimates for the TOA. Originally, these algorithms are usually used for estimating the DOA (Direction-of-arrival). It has been shown in previous papers that they can also be used for estimating the TOA as well as DOA [3, 5, 25–33].

Once the initial TOA estimates are available, it is shown in this paper that the Newton-type nonlinear iteration [10–12] can be applied to refine the initial TOA estimates to get more accurate final TOA estimates.

In the viewpoint of the resolution, the MUSIC algorithm beats the conventional beamforming algorithm. The cost for more accurate estimate of the MUSIC algorithm over the conventional beamforming algorithm is that the MUSIC algorithm is computationally more intensive than the conventional beamforming algorithm. The additional computation required for the implementation of the MUSIC algorithm with respect to the conventional MUSIC algorithm is the calculation of the eigenvectors of the covariance matrix.

In the numerical results, we investigated the effect of the number of the multipath components on the performance the TOA estimation. Although it is true that the performance degrades for large number of the multipath components, it has been shown that the scheme still

works when the number of TOA's is greater than two.

2. BEAMFORMING AND MUSIC ALGORITHM FOR TIME DELAY ESTIMATION [3]

The impulse response of the multipath channel can be written as

$$h(t) = \sum_{k=0}^{L_p} \alpha_k \delta(t - \tau_k) \tag{1}$$

where L_p is the number of multipath, and α_k and τ_k are the amplitude and phase of the k-th multipath component.

Using the Fourier transform of (1), we have the frequency response

$$H(f) = \sum_{k=0}^{L_p} \alpha_k e^{-j2\pi f \tau_k}. \tag{2}$$

Considering the additive Gaussian noise, we can rewrite (2) as

$$x(f) = \sum_{k=0}^{L_p} \alpha_k e^{-j2\pi f \tau_k} + W(f) \tag{3}$$

where $W(f)$ represents additive white Gaussian noise with variance σ_w^2.

Sampling the frequency response at discrete frequency at $f = f_l \equiv f_0 + l\Delta f$ results in

$$x(f_l) = H(f_l) + w(f_l) = \sum_{k=0}^{L_p} \alpha_k e^{-j2\pi f_l \tau_k} + w(f_l) \quad l = 0, \ldots, L-1. \tag{4}$$

Note that L_p is the number of multipath and that L is the number of frequencies considered at which we compute the frequency response.

Using vector notation, (4) can be written as

$$\mathbf{x} = \mathbf{H} + \mathbf{w} = \mathbf{V}\mathbf{a} + \mathbf{w} \tag{5}$$

where

$$\begin{aligned}
\mathbf{H} &= \left[\begin{array}{cccc} H(f_0) & H(f_1) & \ldots & H(f_{L-1}) \end{array}\right]^T \\
\mathbf{w} &= \left[\begin{array}{cccc} w(0) & w(1) & \ldots & w(L-1) \end{array}\right]^T \\
\mathbf{V} &= \left[\begin{array}{cccc} \mathbf{v}(\tau_0) & \mathbf{v}(\tau_1) & \ldots & \mathbf{v}(\tau_{L-1}) \end{array}\right] \\
\mathbf{v}(\tau_k) &= \left[\begin{array}{cccc} 1 & e^{-j2\pi\Delta f \tau_k} & \ldots & e^{-j2\pi(L-1)\Delta f \tau_k} \end{array}\right]^T. \\
\mathbf{a} &= \left[\begin{array}{cccc} \alpha'_0 & \alpha'_1 & \ldots & \alpha'_{L_p-1} \end{array}\right]^T \\
\alpha'_k &= \alpha_k e^{-2\pi f_0 \tau_k}
\end{aligned} \tag{6}$$

Exchanging the time and frequency variables in (2), we have

$$H(\tau) = \sum_{k=0}^{L_p} \alpha_k e^{-j2\pi f_k \tau} \tag{7}$$

which is harmonic model. It has been shown that any spectral estimation techniques for the harmonic signal analysis can also be applied to the TOA estimation using the frequency response [3].

From the explanation in the previous paragraph, the beamforming algorithm can also be used for the estimation of TOA [2, 3]. TOA (Time-of-arrival) can be selected from the delay at which the following output achieves the maximum

$$P_{BF}(\tau) = \mathbf{v}(\tau)^T \mathbf{R} \mathbf{v}(\tau). \tag{8}$$

where τ is the time delay of an interest, $\mathbf{R}$ is the autocorrelation matrix defined from (5)

$$\mathbf{R} = \mathbf{V} E\left\{\mathbf{a}\mathbf{a}^H\right\} \mathbf{V}^H + \sigma_w^2 \mathbf{I} = E\left\{\mathbf{x}\mathbf{x}^H\right\} = \mathbf{V}\mathbf{A}\mathbf{V}^H + \sigma_w^2 \mathbf{I}, \tag{9}$$

and $\mathbf{v}(\tau)$ is given by

$$\mathbf{v}(\tau) = \begin{bmatrix} 1 & e^{-j2\pi\Delta f\tau} & \dots & e^{-j2\pi(L-1)\Delta f\tau} \end{bmatrix}^T. \tag{10}$$

That is, we evaluate (8) as a function of τ at discrete values, and find τ at which $P_{BF}(\tau)$ achieves the maximum:

$$\hat{\tau}_{BF}^{(0)} = \arg\left\{\max_{\tau}\left[P_{BF}(\tau)\right]\right\} = \arg\left\{\max_{\tau}\left[\mathbf{v}(\tau)^T \mathbf{R} \mathbf{v}(\tau)\right]\right\}$$

$$\tau = \tau_{\text{start}}, \tau_{\text{start}} + \Delta\tau, \tau_{\text{start}} + 2\Delta\tau, \dots \tau_{\text{start}} + \left\lfloor \frac{\tau_{\text{stop}} - \tau_{\text{start}}}{\Delta\tau} \right\rfloor \Delta\tau \tag{11}$$

where $\Delta\tau$ is the search increment.

Similarly, using the MUSIC pseudospectrum for TOA estimation can be written as follows:

$$P_{\text{MU}}(\tau) = \frac{1}{\mathbf{v}(\tau)^T \mathbf{P}_w \mathbf{v}(\tau)} \equiv \frac{1}{D_{\text{MU}}(\tau)}. \tag{12}$$

The matrix $\mathbf{P}_w$ can be written as

$$\mathbf{P}_w = \mathbf{U}_N \mathbf{U}_N^H$$

where $\mathbf{U}_N$ is defined using the noise eigenvectors of the covariance matrix $\mathbf{R}$:

$$\mathbf{U}_N = \left[\mathbf{u}_{L_p+1},\ \mathbf{u}_{L_p+2},\ \dots,\ \mathbf{u}_L\right]$$

MUSIC — based TOA's can be determined from the delay values achieving the maximum:

$$\hat{\tau}_{\text{MUSIC}}^{(0)} = \arg\left\{\max_{\tau}\left[P_{\text{MUSIC}}(\tau)\right]\right\} = \arg\left\{\min_{\tau}\left[\mathbf{v}(\tau)^T\mathbf{P}_w\mathbf{v}(\tau)\right]\right\}$$
$$\tau = \tau_{\text{start}}, \tau_{\text{start}} + \Delta\tau, \tau_{\text{start}} + 2\Delta\tau, \ldots \tau_{\text{start}} + \left\lfloor \frac{\tau_{\text{stop}} - \tau_{\text{start}}}{\Delta\tau} \right\rfloor \Delta\tau \quad (13)$$

Note that $\mathbf{v}(\tau)^T\mathbf{P}_w\mathbf{v}(\tau)$ should be minimized over τ, rather than maximized, because it is in the denominator of P_{MUSIC} (τ).

In implementation of beamforming-based TOA, the TOA estimate is determined from the peak value of (8) not at continuous delays but at discrete delays. Therefore, the estimate is inevitably restricted to one of discrete delays at which we compute (8). Of course, this problem can be mitigated by decreasing the increment between the discrete delays, which results in the increase of the computational cost of the beamforming algorithm since the beamforming output should be computed at more discrete delays. This is due to the fact that, given the delay range of interest, decreasing the increment between the discrete delays implies the increase of the number of discrete delays.

3. PROPOSED ALGORITHM

3.1. Beamforming Algorithm

Using (10) in (8), after some manipulation, we have

$$P_{BF}(\tau) = \sum_{m=1}^{L}\sum_{n=1}^{L} e^{j(m-n)2\pi\Delta f\tau} \cdot \mathbf{R}_{nm} \quad (14)$$

where $\mathbf{R}_{nm}$ denotes the n-th row and m-th column of the matrix $\mathbf{R}$.

Although, in the derivation of the scheme, for simplicity, we assume that the number of TOA parameters to be estimated, L_p, is one, it can be also applied to the case of $L_p \geq 2$, which is verified in the numerical results where we try to estimate two parameters of τ_1 and τ_2.

The initial estimate of the TOA, $\hat{\tau}_{BF}^{(0)}$, can be found from (11). To further refine the initial estimate, we have to find the delay which maximizes (14), which is equivalent to finding the delay at which the derivative of (14) is zero.

Differentiation of (14) with respect to τ is easily obtained as

follows:

$$f_{BF}(\tau) \equiv P'_{BF}(\tau) = \frac{P_{BF}(\tau)}{d\tau} = \frac{d}{d\tau}\sum_{m=1}^{L}\sum_{n=1}^{L} e^{j(m-n)2\pi\Delta f\tau}\mathbf{R}_{nm}$$

$$= \sum_{m=1}^{L}\sum_{n=1}^{L} j(m-n)2\pi\Delta f \cdot e^{j(m-n)2\pi\Delta f\tau}\mathbf{R}_{nm}. \quad (15)$$

Since (15) is the derivative of (14), to find the delay which maximizes (14), we have to find the solution of

$$f_{BF}(\tau) = \sum_{m=1}^{L}\sum_{n=1}^{L} j(m-n)2\pi\Delta f \cdot e^{j(m-n)2\pi\Delta f\tau}\mathbf{R}_{nm} = 0. \quad (16)$$

Since the maximum of (14) is obtained from the solution of (16), the initial guess of the solution of (16) is the initial TOA estimate of (14). As previously stated, since the initial TOA estimate is obtained from (11), the initial guess of the solution of (16) is also calculated from (11).

Our concern is, given the initial estimate, $\hat{\tau}_{BF}^{(0)}$, how to find the solution of (16) numerically. The final estimate, $\hat{\tau}_{BF}^{(\text{final})}$, can be obtained from the iterative update. To find the solution of (16) using the Newton iteration, we have to find the derivative of $f_{BF}(\tau)$ with respect to τ.

The derivative of (7) is easily obtained to be

$$f'_{BF}(\tau) = \sum_{m=1}^{L}\sum_{n=1}^{L} (j(m-n)2\pi\Delta f)^2 \cdot e^{j(m-n)2\pi\Delta f\tau} \cdot \mathbf{R}_{nm} \quad (17)$$

Using (15) and (17), the following iteration is repeated until the update of the estimate is less than the specified tolerance. That is, when the update of the estimate, $\left|\hat{\tau}_{BF}^{(i+1)} - \hat{\tau}_{BF}^{(i)}\right|$, is less than the specified tolerance, the estimate is considered to be convergent.

$$\hat{\tau}_{BF}^{(i+1)} = \hat{\tau}_{BF}^{(i)} - \frac{f(\hat{\tau}_{BF}^{(i)})}{f'(\hat{\tau}_{BF}^{(i)})}$$

$$= \hat{\tau}_{BF}^{(i)} - \frac{\sum_{m=1}^{L}\sum_{n=1}^{L} j(m-n)2\pi\Delta f \cdot e^{j(m-n)2\pi\Delta f\hat{\tau}_{BF}^{(i)}}\mathbf{R}_{nm}}{\sum_{m=1}^{L}\sum_{n=1}^{L} (j(m-n)2\pi\Delta f)^2 \cdot e^{j(m-n)2\pi\Delta f\hat{\tau}_{BF}^{(i)}} \cdot \mathbf{R}_{nm}} \quad i=0,1,\ldots (18)$$

where the initial estimate $\hat{\tau}_{BF}^{(0)}$ used for the first iteration is obtained from (4), and $\hat{\tau}_{BF}^{(i)}$ represents the TOA estimate for the i-th iteration. The estimate obtained from the last iteration is designated as the final estimate $\hat{\tau}_{BF}^{(\text{final})}$.

3.2. MUSIC Algorithm

Using (10) in (12), after some manipulation, we have

$$P_{\text{MU}}(\tau) = \frac{1}{\sum\limits_{m=1}^{L}\sum\limits_{n=1}^{L} e^{j(m-n)2\pi\Delta f\tau} \cdot \mathbf{P}_{w\,nm}} \equiv \frac{1}{D_{\text{MU}}(\tau)}. \tag{19}$$

Following the way how we refine the initial estimate which has been obtained using the beamforming algorithm, we can easily find how we can refine the initial estimate obtained from the MUSIC algorithm.

We have to find the delay which maximizes $P_{\text{MU}}(\tau)$, which is equivalent to finding the delay where $D_{\text{MU}}(\tau)$ can be minimized.

The delay minimizing $D_{\text{MU}}(\tau)$ can also be found from the values where the derivative of $D_{\text{MU}}(\tau)$ is zero.

Differentiation of $D_{\text{MU}}(\tau)$ with respect to τ is easily obtained as follows:

$$\begin{aligned} f_{\text{MU}}(\tau) \equiv D'_{\text{MU}}(\tau) &= \frac{D_{\text{MU}}(\tau)}{d\tau} = \frac{d}{d\tau}\sum_{m=1}^{L}\sum_{n=1}^{L} e^{j(m-n)2\pi\Delta f\tau}\mathbf{P}_{w\,nm} \\ &= \sum_{m=1}^{L}\sum_{n=1}^{L} j(m-n)2\pi\Delta f \cdot e^{j(m-n)2\pi\Delta f\tau}\mathbf{P}_{w\,nm} \end{aligned} \tag{20}$$

We have to find the solution of

$$f_{\text{MU}}(\tau) = \sum_{m=1}^{L}\sum_{n=1}^{L} j(m-n)2\pi\Delta f \cdot e^{j(m-n)2\pi\Delta f\tau}\mathbf{P}_{w\,nm} = 0. \tag{21}$$

Our concern is, given the initial estimate, $\hat{\tau}_{\text{MU}}^{(0)}$, how to find the solution of (21) numerically. To find the final estimate, $\hat{\tau}_{\text{MU}}^{(\text{final})}$, we have to find the derivative of $f_{\text{MU}}(\tau)$ with respect to τ.

The derivative of (21) can be written as

$$f'_{\text{MU}}(\tau) = \sum_{m=1}^{L}\sum_{n=1}^{L} (j(m-n)2\pi\Delta f)^2 \cdot e^{j(m-n)2\pi\Delta f\tau} \cdot \mathbf{P}_{w\,nm} \tag{22}$$

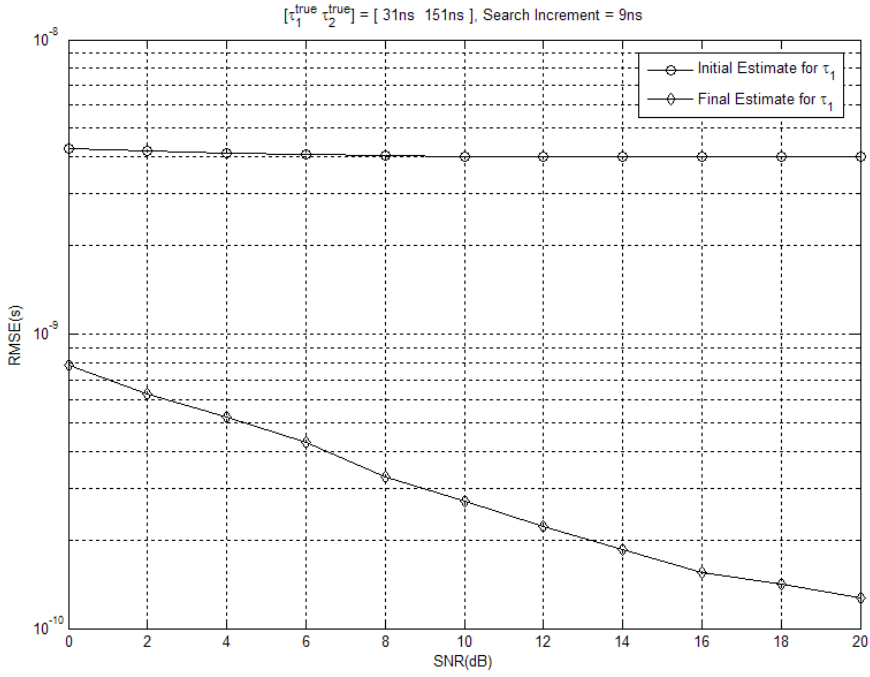

Figure 1. Initial and final estimates of the first delay obtained from the beamforming algorithm for two TOA's ($[\hat{\tau}_1^{(\text{true})} \;\; \hat{\tau}_2^{(\text{true})}] = [31\text{ ns } 151\text{ ns}],\ \Delta\tau = 9\,\text{ns}$).

Using (20) and (22), the following iteration is repeated until convergence is achieved

$$\hat{\tau}_{\text{MU}}^{(i+1)} = \hat{\tau}_{\text{MU}}^{(i)} - \frac{f\left(\hat{\tau}_{\text{MU}}^{(i)}\right)}{f'\left(\hat{\tau}_{\text{MU}}^{(i)}\right)} =$$

$$\hat{\tau}_{\text{MU}}^{(i)} - \frac{\sum_{m=1}^{L}\sum_{n=1}^{L} j(m-n)2\pi\Delta f \cdot e^{j(m-n)2\pi\Delta f\hat{\tau}_{\text{MU}}^{(i)}}\mathbf{P}_{w\,nm}}{\sum_{m=1}^{L}\sum_{n=1}^{L}\left(j(m-n)2\pi\Delta f\right)^2 \cdot e^{j(m-n)2\pi\Delta f\hat{\tau}_{\text{MU}}^{(i)}} \cdot \mathbf{P}_{w\,nm}} \quad i=0,1,\ldots \quad (23)$$

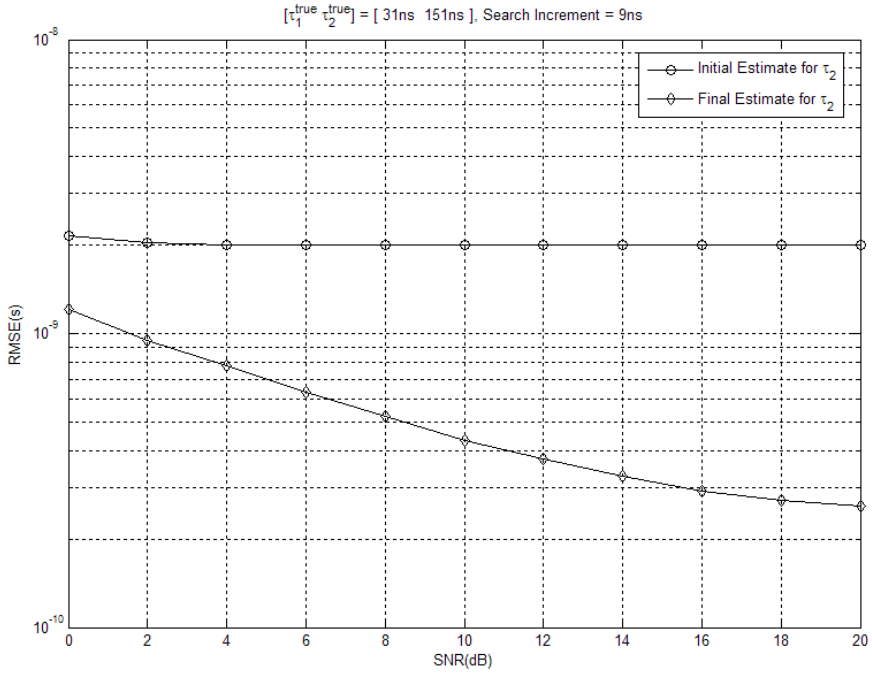

Figure 2. Initial and final estimates of the second delay obtained from the beamforming algorithm for two TOA's $([\hat{\tau}_1^{(\text{true})} \ \hat{\tau}_2^{(\text{true})}] = [31\text{ ns } 151\text{ ns}],\ \Delta\tau = 9\,\text{ns})$.

4. NUMERICAL RESULTS

The discrete data are obtained from sampling the frequency response at equally spaced frequencies. The center frequency is $f_0 = 10^9\,\text{Hz}$, and the bandwidth is given by $20 \times 10^6\,\text{Hz}$. The frequency step for sampling frequency response is $\Delta f = 10^6\,\text{Hz}$. Thus, the frequencies considered are given by

$$f_l = \left(10^9 - 10 \times 10^6\right) + 10^6 \times l \quad l = 0, \ldots, 20. \tag{24}$$

The frequency responses are generated using (5) and L is given by $L = 21$.

In this section, the numerical results are provided to validate the proposed scheme. In Figs. 1–14, it is assumed that we want to estimate two delay parameters of τ_1 and τ_2, which indicates $L_p = 2$ in (1). The amplitudes of the first multipath and that of the second multipath are

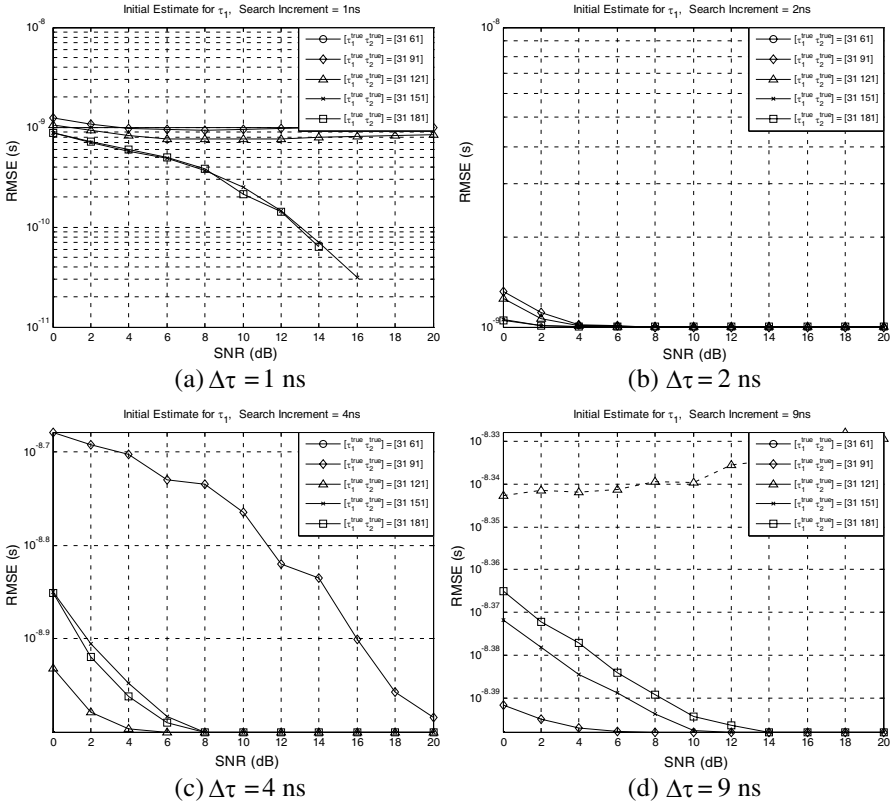

(a) $\Delta\tau = 1$ ns (b) $\Delta\tau = 2$ ns

(c) $\Delta\tau = 4$ ns (d) $\Delta\tau = 9$ ns

Figure 3. Initial estimates of the first delay obtained from the beamforming algorithm for two TOA's.

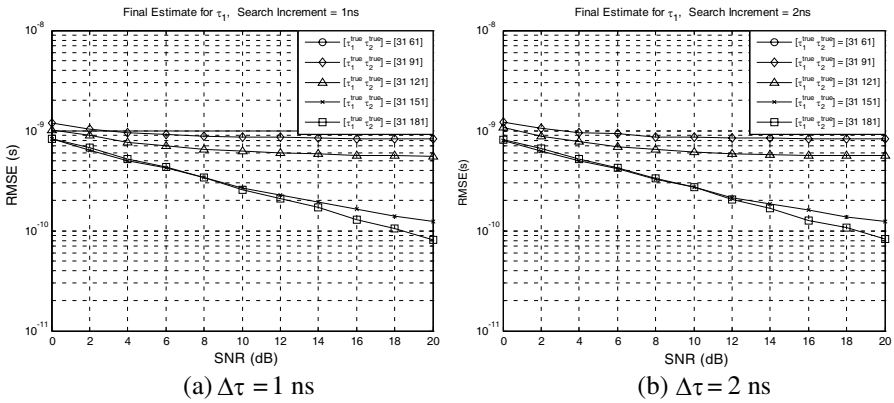

(a) $\Delta\tau = 1$ ns (b) $\Delta\tau = 2$ ns

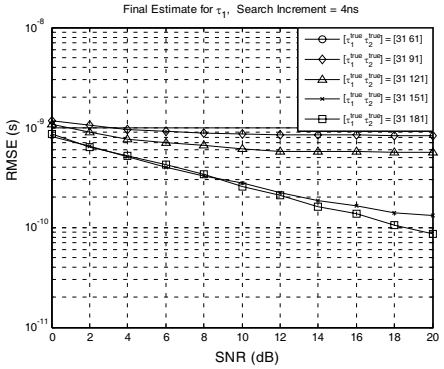

(c) $\Delta\tau = 4$ ns

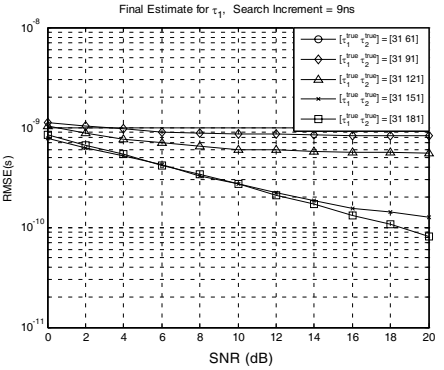

(d) $\Delta\tau = 9$ ns

Figure 4. Final estimates of the first delay obtained from the beamforming algorithm for two TOA's.

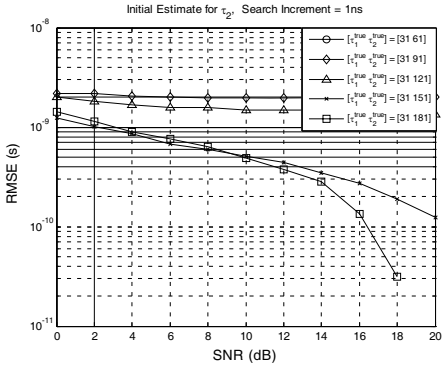

(a) $\Delta\tau = 1$ ns

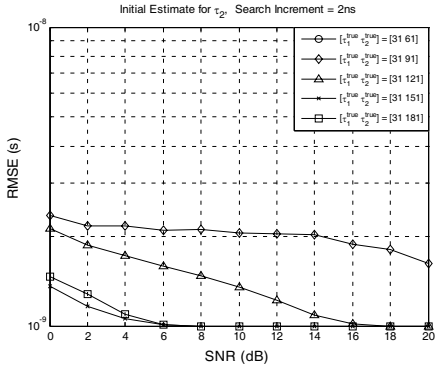

(b) $\Delta\tau = 2$ ns

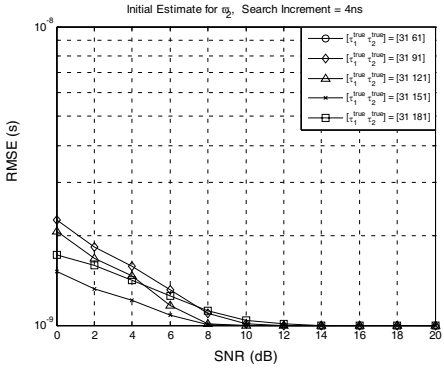

(c) $\Delta\tau = 4$ ns

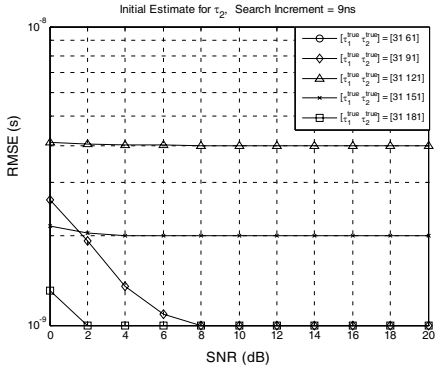

(d) $\Delta\tau = 9$ ns

Figure 5. Initial estimates of the second delay obtained from the beamforming algorithm for two TOA's.

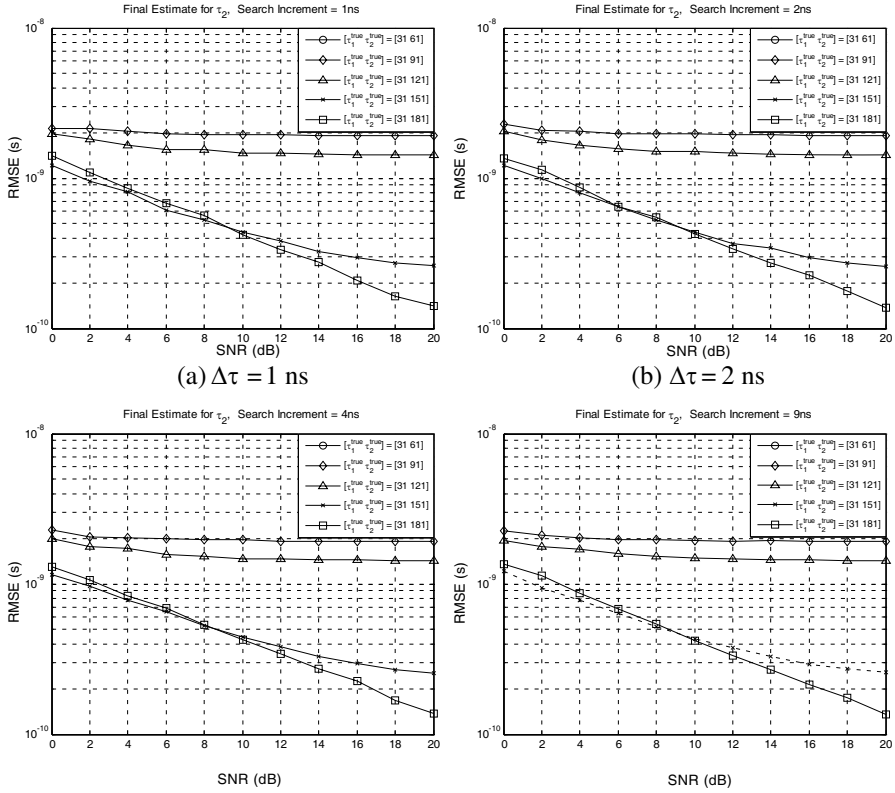

(a) $\Delta\tau = 1$ ns (b) $\Delta\tau = 2$ ns

(c) $\Delta\tau = 4$ ns (d) $\Delta\tau = 9$ ns

Figure 6. Final estimates of the second delay obtained from the beamforming algorithm for two TOA's.

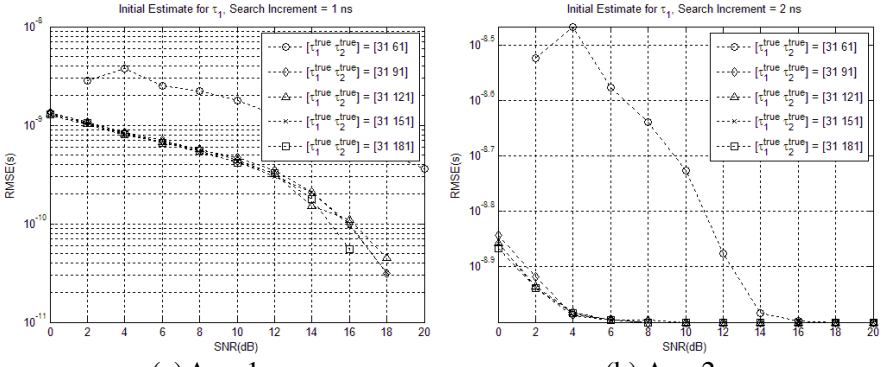

(a) $\Delta\tau = 1$ ns (b) $\Delta\tau = 2$ ns

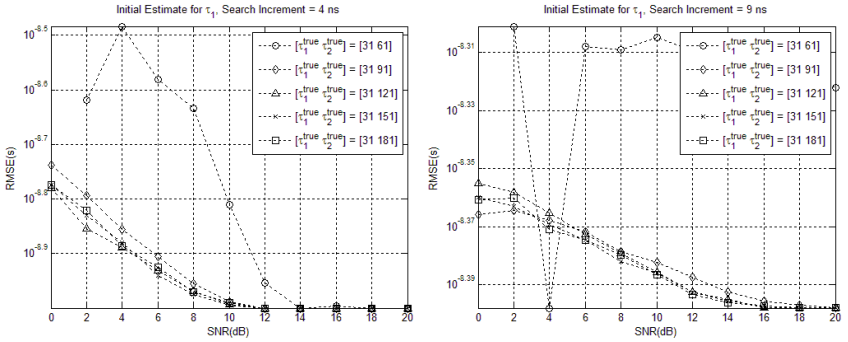

(c) $\Delta\tau = 4$ ns (d) $\Delta\tau = 9$ ns

Figure 7. Initial estimates of the first delay obtained from the MUSIC algorithm for two TOA's.

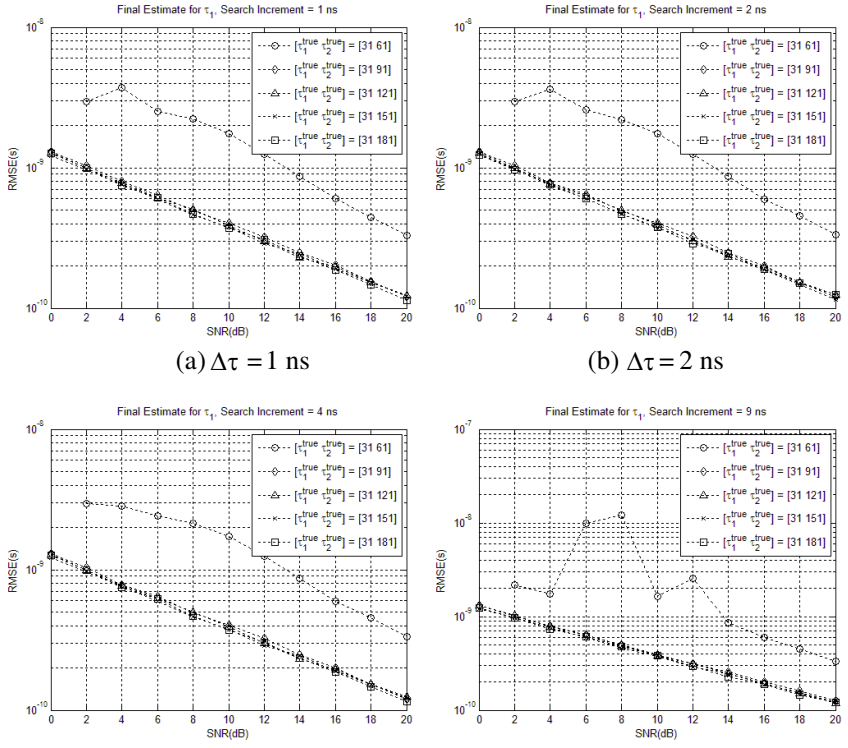

(a) $\Delta\tau = 1$ ns (b) $\Delta\tau = 2$ ns

(c) $\Delta\tau = 4$ ns (d) $\Delta\tau = 9$ ns

Figure 8. Final estimates of the first delay obtained from the MUSIC algorithm for two TOA's.

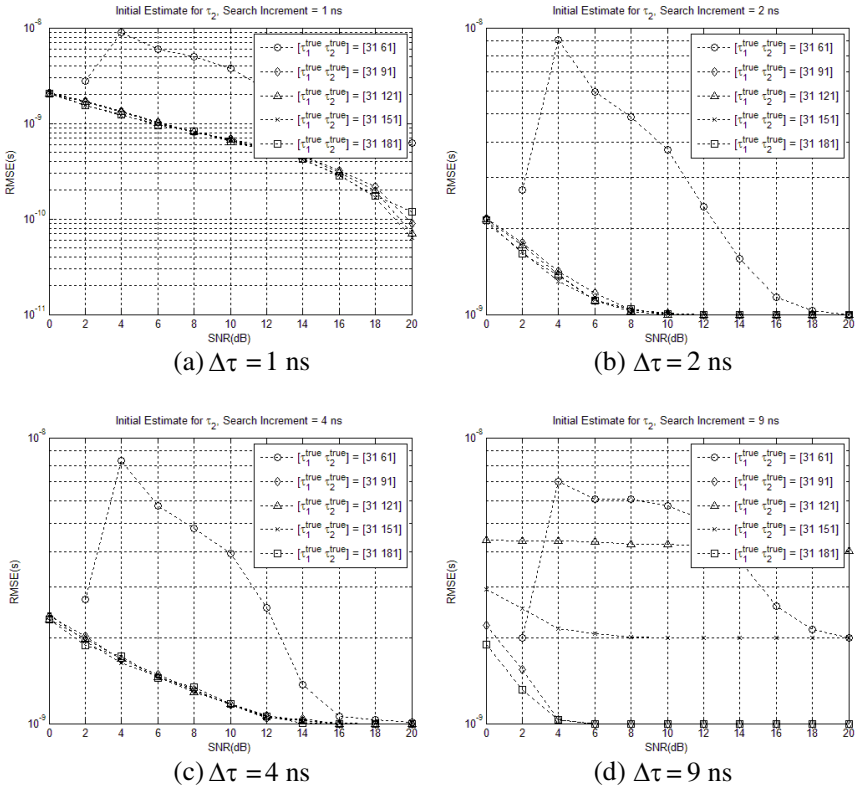

(a) $\Delta\tau = 1$ ns (b) $\Delta\tau = 2$ ns

(c) $\Delta\tau = 4$ ns (d) $\Delta\tau = 9$ ns

Figure 9. Initial estimates of the second delay obtained from the MUSIC algorithm for two TOA's.

chosen to be 1 and 0.8, respectively. In Figs. 15–18, L_p can be $L_p = 2$ or $L_p = 10$, and in Figs. 19–30, L_p is equal to three.

The Root-Mean-Square Error (RMSE) is used as a criterion for the estimate accuracy. RMSE is calculated from Ntials repetitions as follows:

$$\text{RMSE}\left(\hat{\tau}_i^{(0)}\right) \equiv \sqrt{\frac{\sum_{j=1}^{\text{Ntrials}} \left|\hat{\tau}_{i,j}^{(0)} - \tau_i^{(\text{true})}\right|^2}{\text{Ntrials}}} \quad i = 1, 2, \ldots, L_p \tag{25}$$

$$\text{RMSE}\left(\hat{\tau}_i^{(\text{final})}\right) \equiv \sqrt{\frac{\sum_{j=1}^{\text{Ntrials}} \left|\hat{\tau}_{i,j}^{(\text{final})} - \tau_i^{(\text{true})}\right|^2}{\text{Ntrials}}} \quad i = 1, 2, \ldots, L_p$$

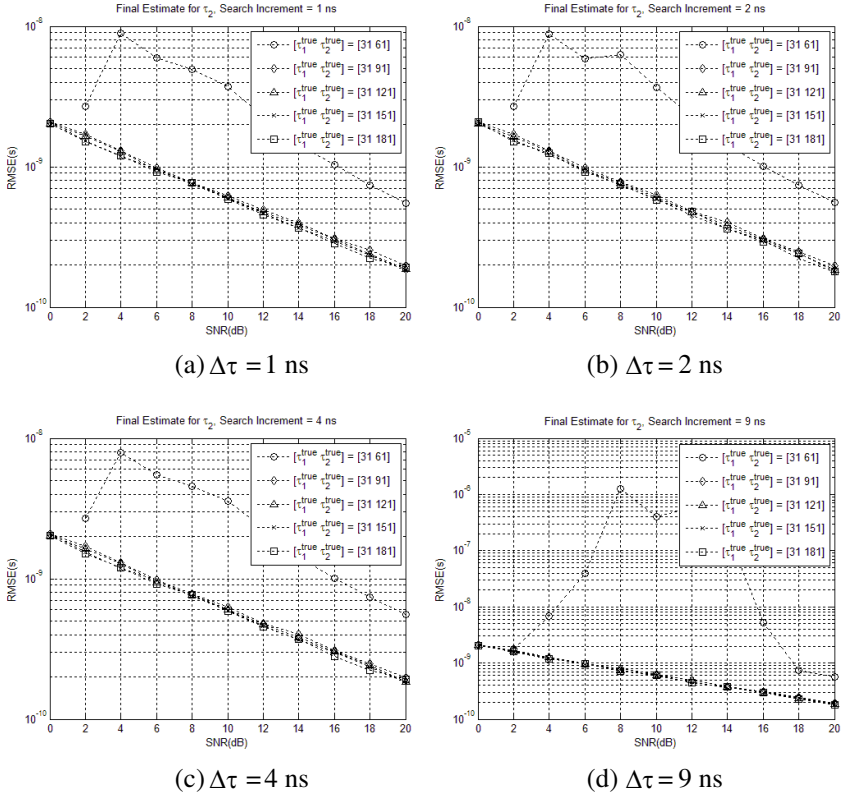

(a) $\Delta\tau = 1$ ns (b) $\Delta\tau = 2$ ns

(c) $\Delta\tau = 4$ ns (d) $\Delta\tau = 9$ ns

Figure 10. Final estimates of the second delay obtained from the MUSIC algorithm for two TOA's.

where subscript j denotes the j-th estimate out of Ntrials = 1000 repetitions, and L_p is the number of the TOA's to be estimated.

Figures 1–2 show the RMSE's of $\hat{\tau}_1^{(0)}$, $\hat{\tau}_1^{(\text{final})}$, $\hat{\tau}_2^{(0)}$ and $\hat{\tau}_2^{(\text{final})}$ for search increment of $\Delta\tau = 9$ ns. The true time delays are given by $\hat{\tau}_1^{(\text{true})} = 31$ ns and $\hat{\tau}_2^{(\text{true})} = 151$ ns. While RMSE's of $\hat{\tau}_1^{(0)}$ are approximately 4×10^{-9}, RMSE of $\hat{\tau}_0^{(\text{final})}$ decreases significantly compared with that of $\hat{\tau}_1^{(0)}$. Therefore, RMSE of $\hat{\tau}_1^{(\text{final})}$ is much less than that of $\hat{\tau}_1^{(0)}$, which validates the proposed scheme. The same is true for $\hat{\tau}_2^{(0)}$ and $\hat{\tau}_2^{(\text{final})}$, which is evident from Fig. 2.

In Figs. 3–6, the parameters for the simulations are the separation between true time delays, $\left|\tau_1^{(\text{true})} - \tau_2^{(\text{true})}\right|$ and the search increment of

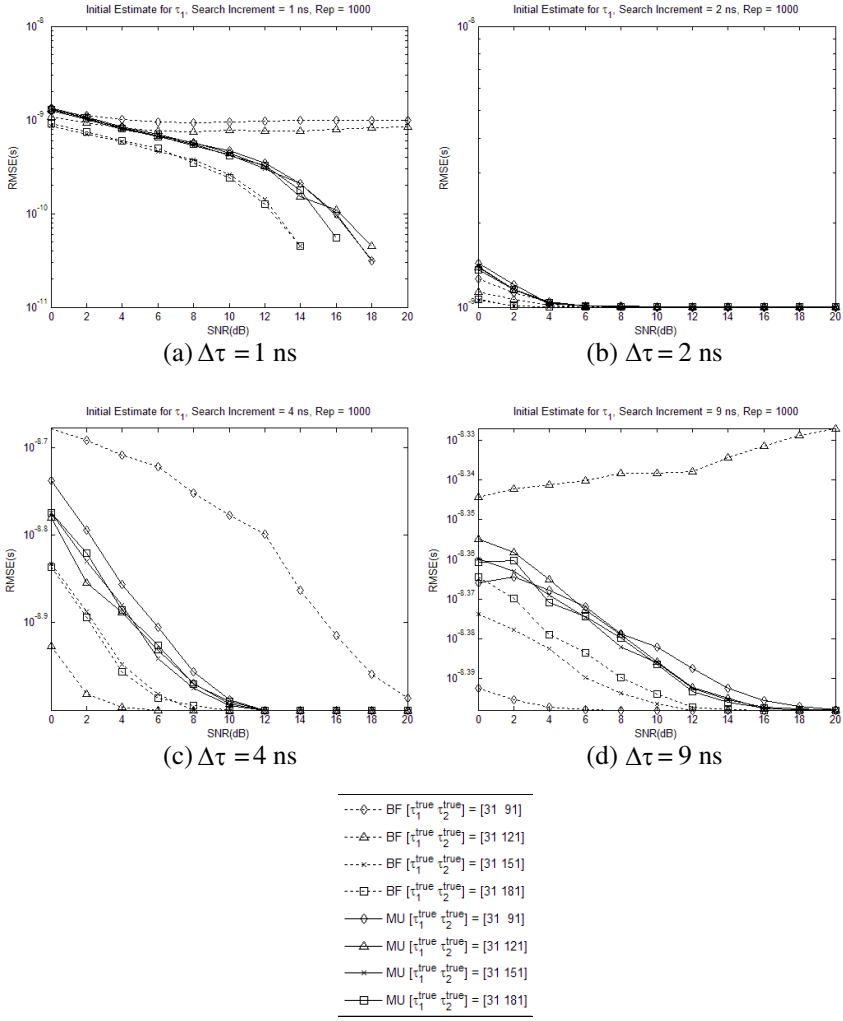

Figure 11. Initial estimates of the first delay for two TOA's.

the discrete time delays, $\Delta\tau$, at which we compute the beamforming output The effects of the search increment, $\Delta\tau$, is illustrated. $\Delta\tau$ values for (a), (b), (c), and (d) are $\Delta\tau = 1\,\text{ns}$, $\Delta\tau = 2\,\text{ns}$, $\Delta\tau = 4\,\text{ns}$ and $\Delta\tau = 9\,\text{ns}$, respectively.

Increasing $\Delta\tau$ results in the reduction in the computational cost of the beamforming algorithm since the beamforming output should be computed at more discrete time delays. This is due to the fact that, given the time delay range of interest, increasing the increment

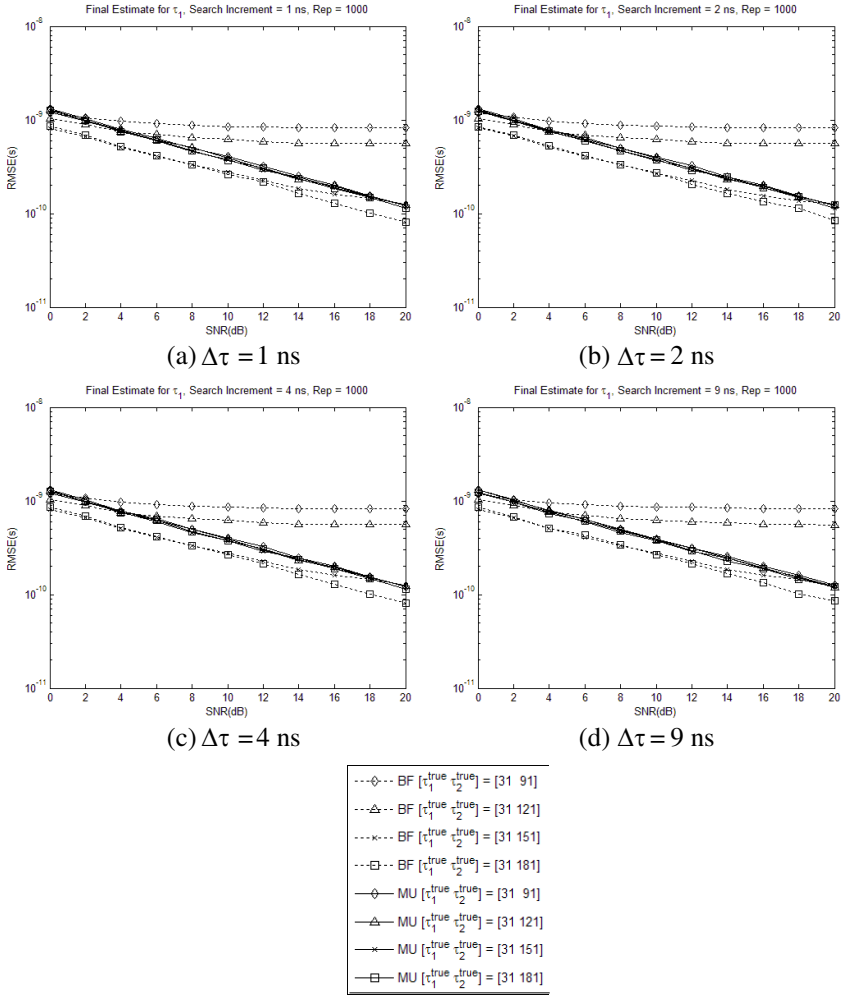

Figure 12. Final estimates of the first delay for two TOA's.

between the discrete time delays implies the decrease in the number of discrete time delays at which we have to evaluate the cost function.

The true time delays are as follows:

$$\left[\begin{array}{cc} \hat{\tau}_1^{(\text{true})} & \hat{\tau}_2^{(\text{true})} \end{array}\right] = [31\,\text{ns} \quad 61\,\text{ns}], [31\,\text{ns} \quad 91\,\text{ns}], [31\,\text{ns} \quad 121\,\text{ns}],$$
$$[\ 31\,\text{ns} \quad 151\,\text{ns}\ ], [\ 31\,\text{ns} \quad 181\,\text{ns}\ ].$$

Therefore, $\left|\tau_1^{(\text{true})} - \tau_2^{(\text{true})}\right|$ values are 30 ns, 60 ns, 90 ns, 120 ns,

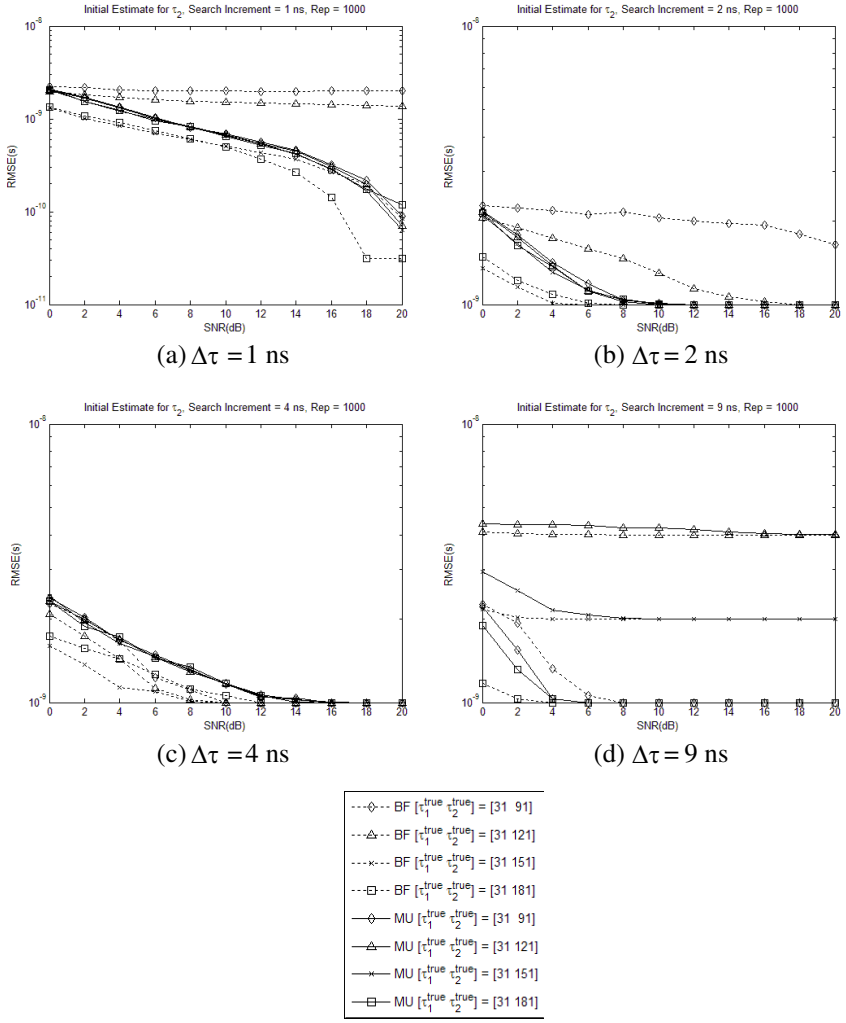

Figure 13. Initial estimates of the second delay for two TOA's.

and 150 ns, respectively. As shown in Figs. 3–6, the RMSE usually decreases as $\left|\tau_1^{(\text{true})} - \tau_2^{(\text{true})}\right|$ increases.

Figures 3, 4, 5 and 6 show the RMSE's of $\hat{\tau}_1^{(0)}$, $\hat{\tau}_1^{(\text{final})}$, $\hat{\tau}_2^{(0)}$ and $\hat{\tau}_2^{(\text{final})}$, respectively. In Figs. 3 and 5, we have shown the results when the Newton iteration is not applied. That is, the results of the beamforming algorithm are displayed. On the other hand, in

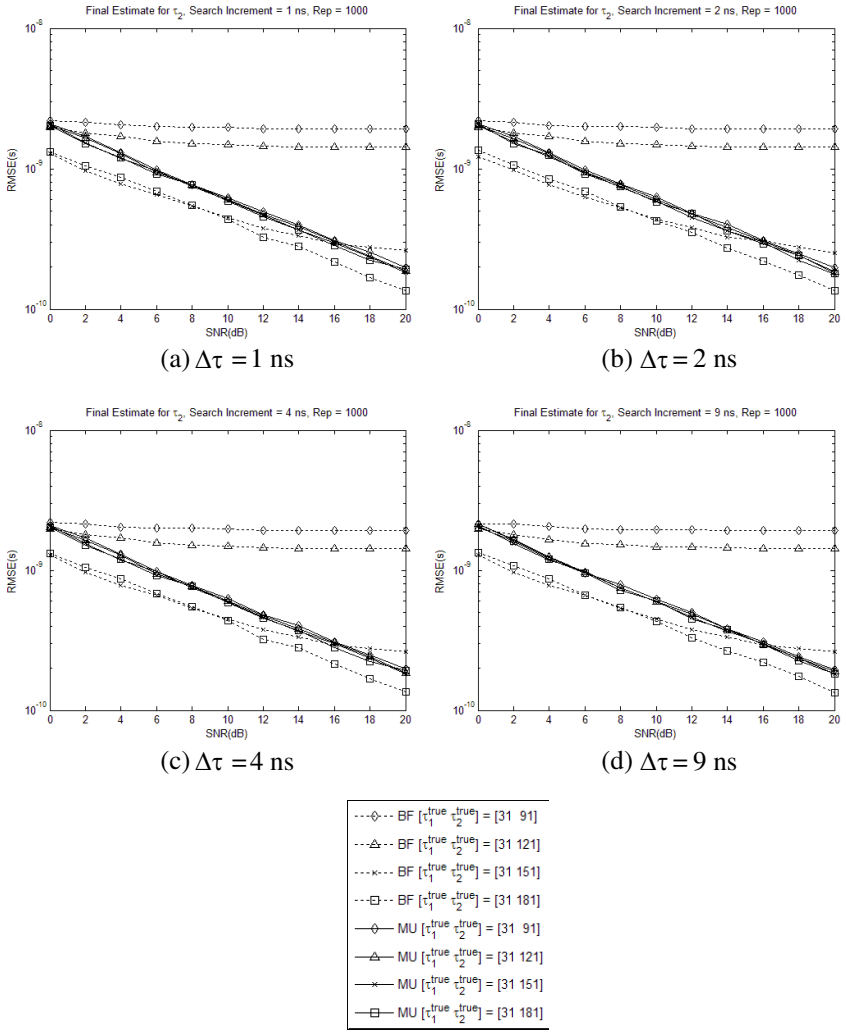

Figure 14. Final estimates of the second delay for two TOA's.

Figs. 4 and 6, the results are shown when the Newton iteration is applied to the initial estimates of the beamforming algorithm. Figs. 3–6 indicate that the proposed scheme can be applied for various values of $\left|\tau_1^{(\text{true})} - \tau_2^{(\text{true})}\right|$ and various values of search increment, $\Delta\tau$.

Comparing Fig. 3 and Fig. 4, it is confirmed that the estimation accuracy of the first TOA is improved using the Newton iteration. Similarly, from Fig. 5 and Fig. 6, we can see that the Newton method

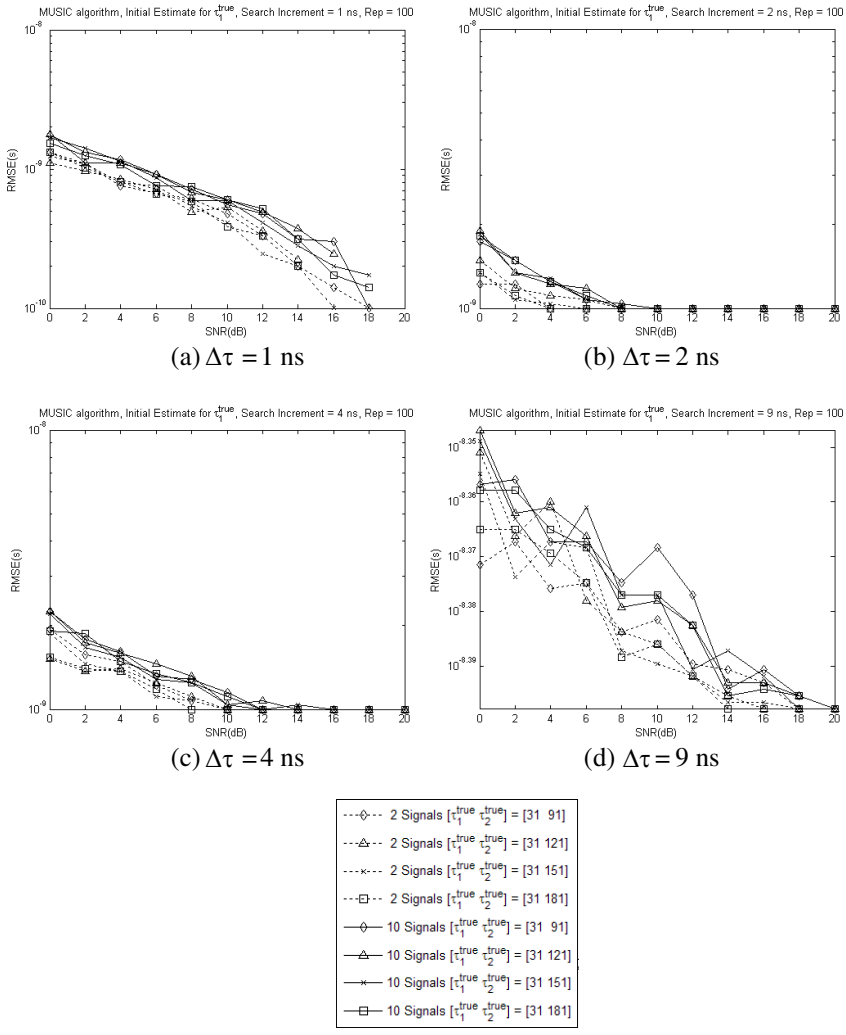

Figure 15. Initial estimates of the first delay obtained from the MUSIC algorithm using (19) for two TOA's and ten TOA's.

results in the accuracy improvement of the estimate of the second TOA.

Note that, in Fig. 3(a), the line corresponding to $[\hat{\tau}_1^{(\text{true})} \ \hat{\tau}_2^{(\text{true})}]$ = [31 ns 61 ns] is not shown for all SNR's and the reason is as follows: Two incident angles are too close to each other to be resolved in the beamforming algorithm. What happens in that case is that we can get only one initial estimate, which usually is located between two

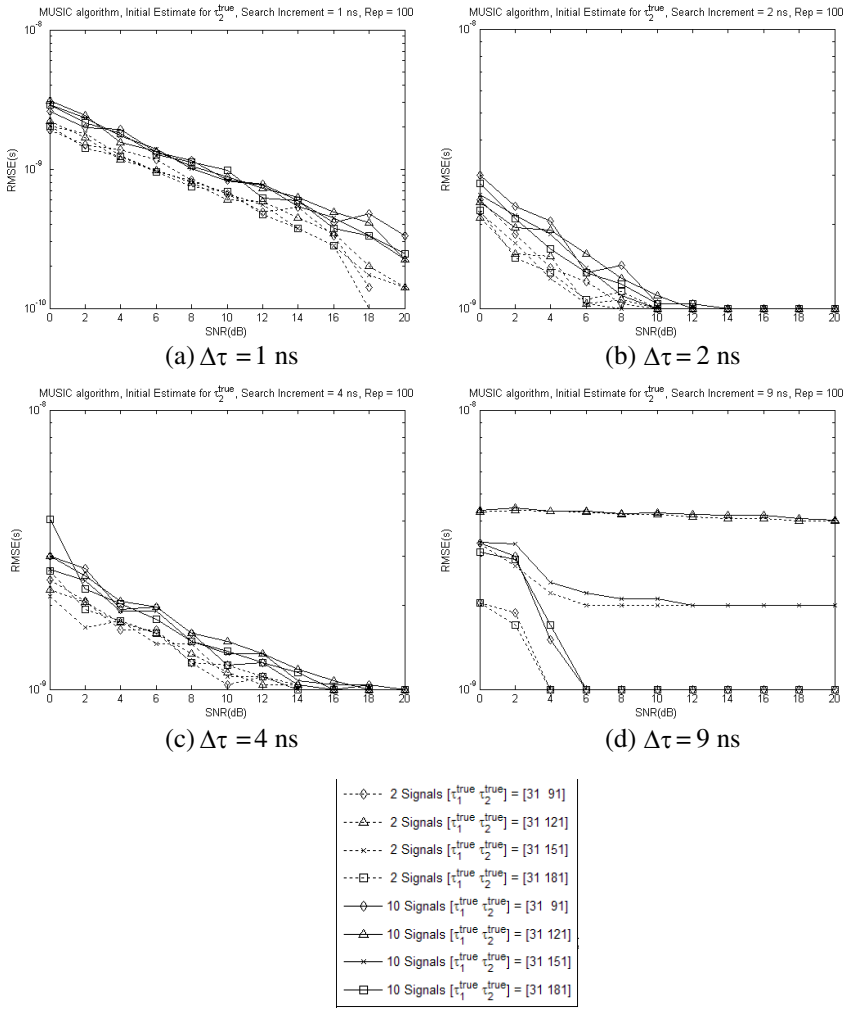

Figure 16. Initial estimates of the second delay obtained from the MUSIC algorithm using (19) for two TOA's and ten TOA's.

true TOA's. Thus, we do not calculate the RMSE's in the case that only one initial estimate is found. That is why there is no result for $[\hat{\tau}_1^{(\text{true})}\ \hat{\tau}_2^{(\text{true})}] = [31\,\text{ns}\ 61\,\text{ns}]$.

On the other hand, in Fig. 7(a), if we use the MUSIC algorithm, the two TOA's can be resolved $[\hat{\tau}_1^{(\text{true})}\ \hat{\tau}_2^{(\text{true})}] = [31\,\text{ns}\ 61\,\text{ns}]$.

Another thing we have to notice in Fig. 3(a) is that there is

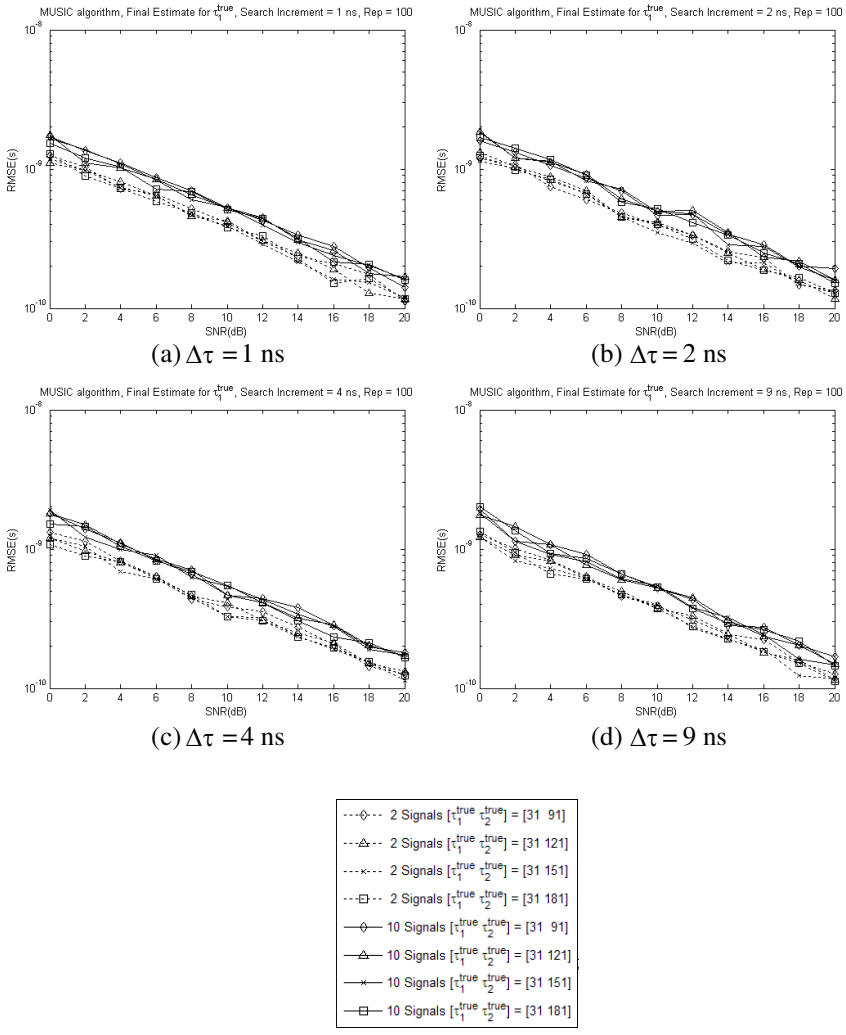

Figure 17. Final estimates of the first delay obtained from the MUSIC algorithm using (23) for two TOA's and ten TOA's.

no result for $[\hat{\tau}_1^{(\text{true})}\ \hat{\tau}_2^{(\text{true})}] = [31\,\text{ns}\ 151\,\text{ns}]$ and SNR = 18, 20 dB. Similarly, there is no result for $[\hat{\tau}_1^{(\text{true})}\ \hat{\tau}_2^{(\text{true})}] = [31\,\text{ns}\ 181\,\text{ns}]$ and SNR = 16, 18, 20 dB. You can easily understand these phenomena from the fact that the search increment for Fig. 3(a) is 1 ns. When the initial estimate obtained from the beamforming algorithm is exactly equal to the true estimate, the RMSE is identically zero. Since the

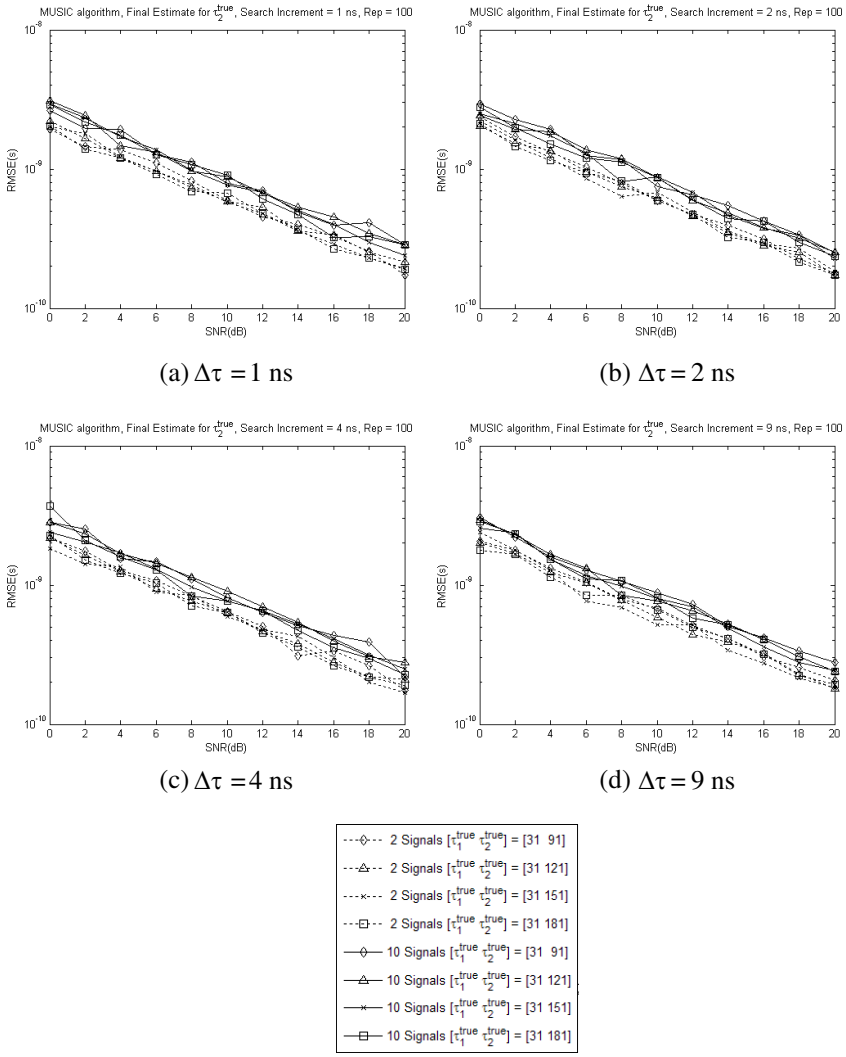

(a) $\Delta\tau = 1$ ns (b) $\Delta\tau = 2$ ns

(c) $\Delta\tau = 4$ ns (d) $\Delta\tau = 9$ ns

Figure 18. Final estimates of the second delay obtained from the MUSIC algorithm using (23) for two TOA's and ten TOA's.

y-axis of the graph is of logarithmic scale, zero cannot be shown in the figure. The same is true for $\left[\hat{\tau}_1^{(\text{true})} \;\; \hat{\tau}_2^{(\text{true})}\right] = [31\,\text{ns}\;\; 181\,\text{ns}]$ and SNR = 20 dB in Fig. 5(a) which shows the results for the second delay.

In Figs. 7–10, we show that our scheme can also be applied to the MUSIC algorithm. It is clearly shown that using initial estimates

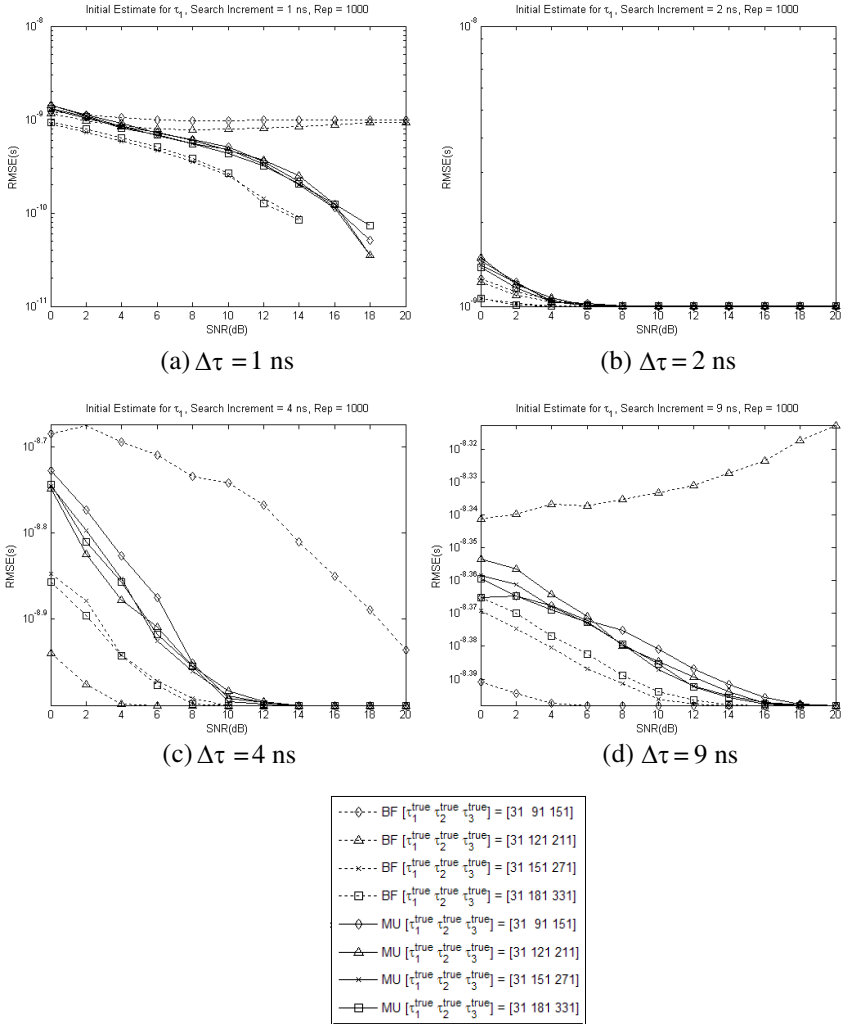

Figure 19. Initial estimates of the first delay obtained from the beamforming algorithm and the MUSIC algorithm when there are three TOA's.

from the MUSIC algorithm, we can get more accurate final estimates by applying the scheme proposed in this paper.

In Figs. 11–14, we compare the initial estimates obtained from the beamforming algorithm with those obtained from the MUSIC algorithm. 'BF' and 'MU' denote the beamforming algorithm and the MUSIC algorithm, respectively. We will summarize a few observations

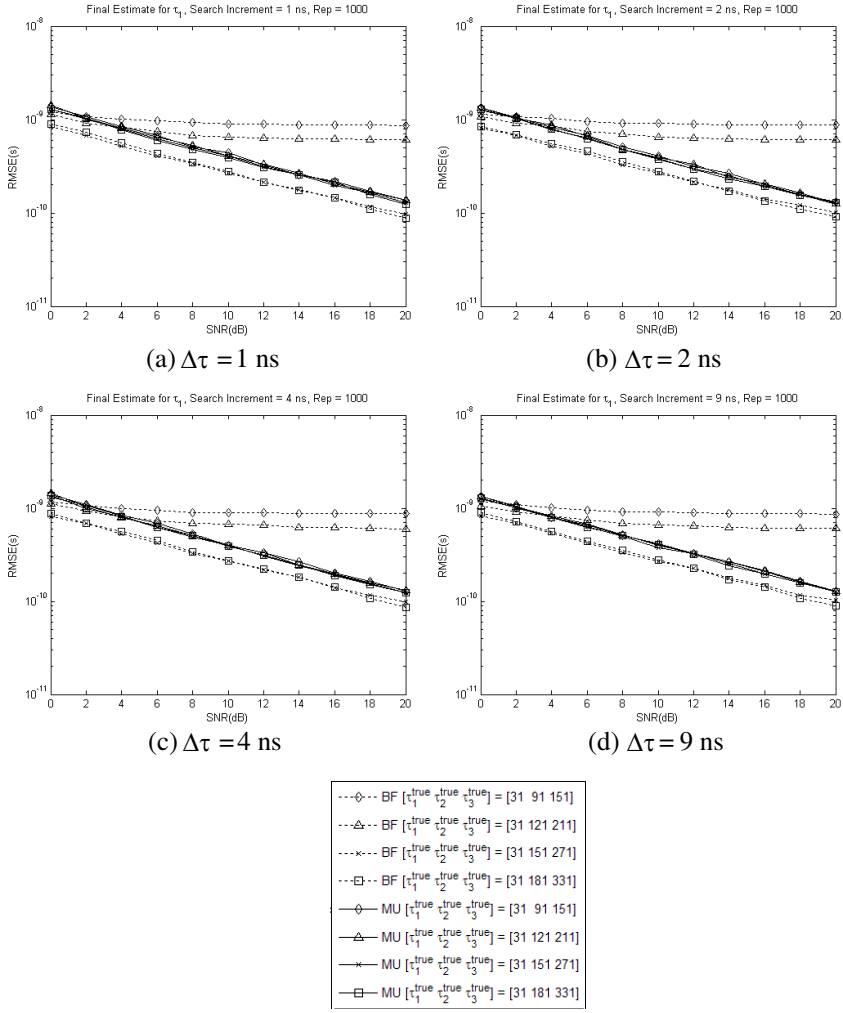

Figure 20. Final estimates of the first delay obtained from the beamforming algorithm and the MUSIC algorithm when there are three TOA's.

in Figs. 11–14.

First, note that it is not always true that the MUSIC algorithm outperforms the beamforming algorithm. The superiority of the MUSIC algorithm to the beamforming algorithm is quite obvious when two true TOA's are close to each other. At low SNR's, it may be true that the beamforming algorithm is better than the MUSIC algorithm,

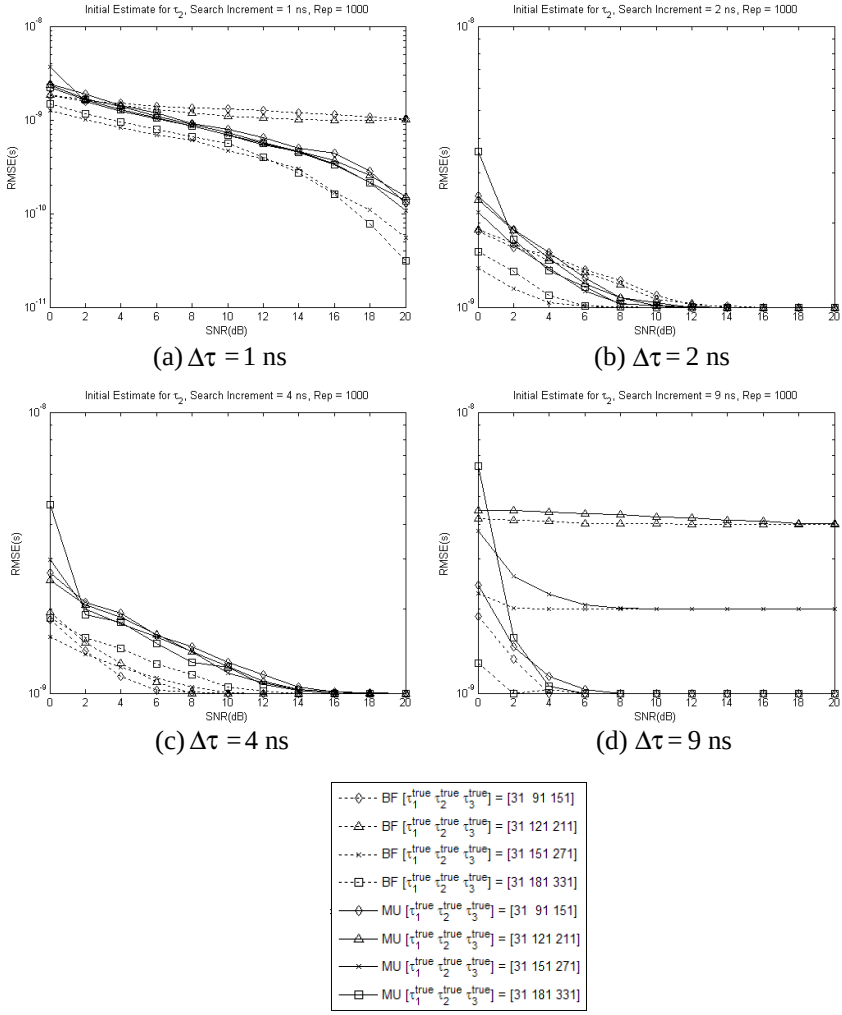

Figure 21. Initial estimates of the second delay obtained from the beamforming algorithm and the MUSIC algorithm when there are three TOA's.

which can be shown in Fig. This phenomenon can be explained from the fact that, in MUSIC algorithm, we have to calculate the noise eigenvector of the noisy covariance matrix which is essentially very ill-conditioned operation.

It is easily observed that, at high SNR's, the Newton iteration proposed in this paper is capable of greatly improving the accuracy

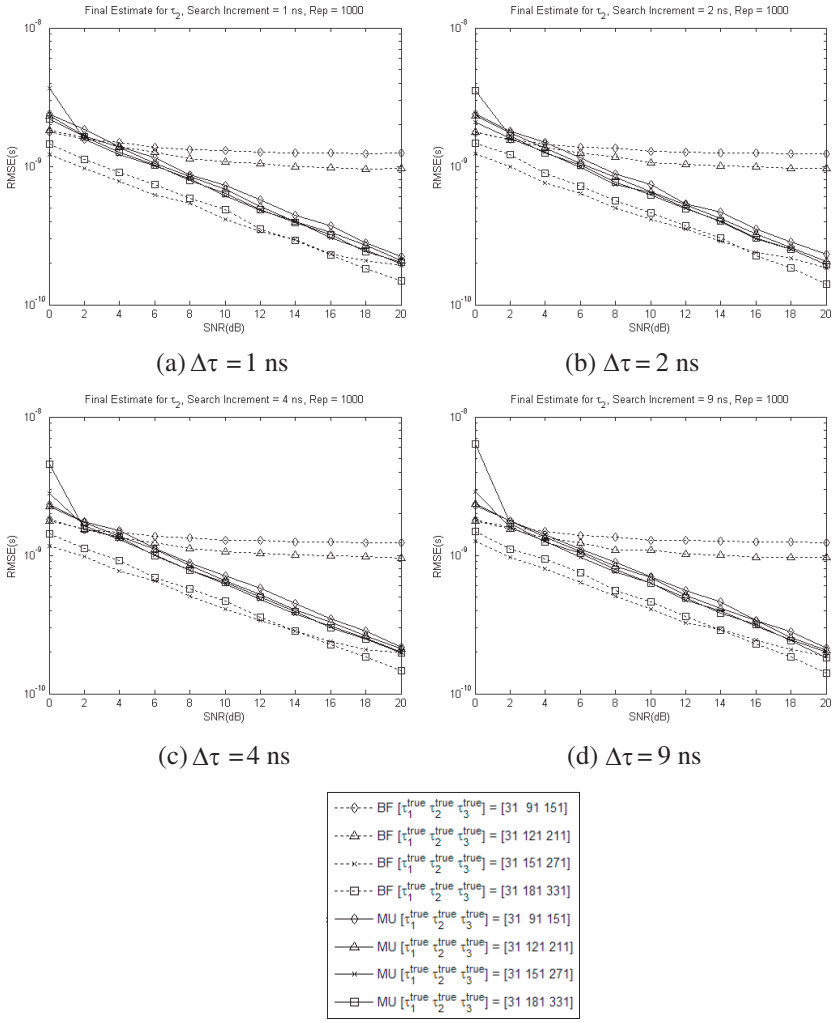

(a) $\Delta\tau = 1$ ns (b) $\Delta\tau = 2$ ns

(c) $\Delta\tau = 4$ ns (d) $\Delta\tau = 9$ ns

Figure 22. Final estimates of the second delay obtained from the beamforming algorithm and the MUSIC algorithm when there are three TOA's.

of the initial estimates both for the beamforming algorithm and the MUSIC algorithm.

In Figs. 15–18, we have considered the case that the number of TOA's is greater than two. We compared the RMS errors when the number of the TOA's is two and ten. We used the MUSIC algorithm.

The solid lines correspond to the case in which we estimate the

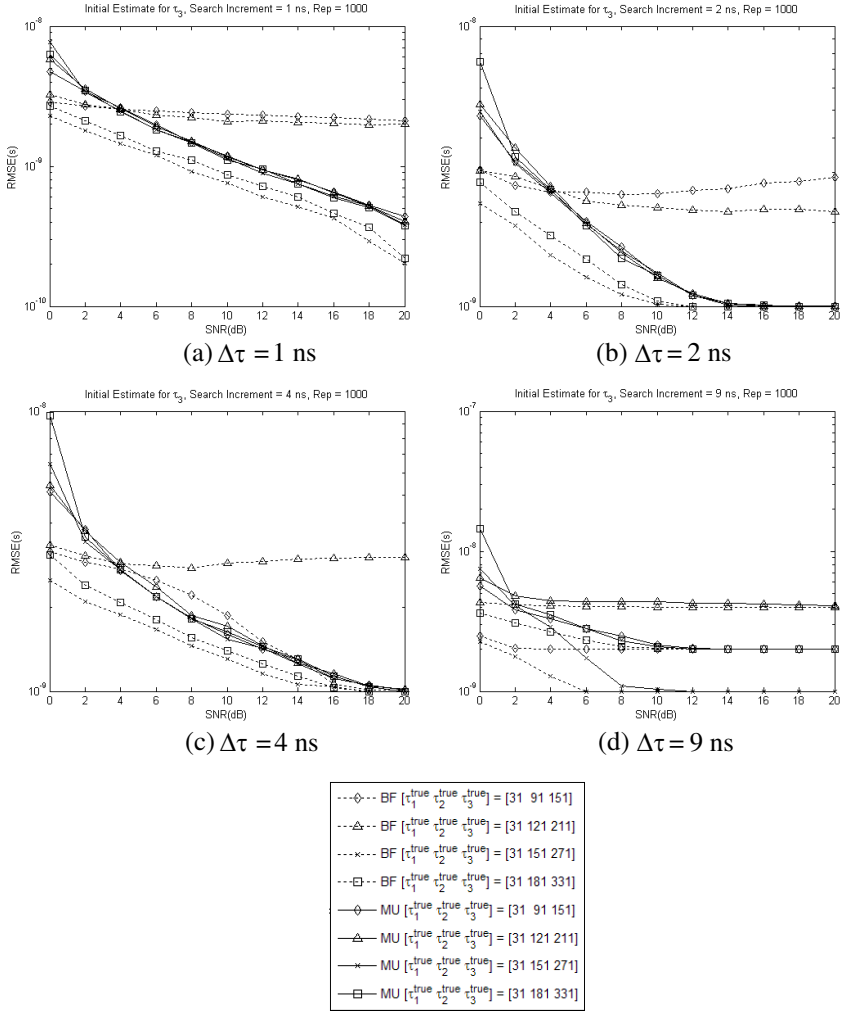

Figure 23. Initial estimates of the third delay obtained from the beamforming algorithm and the MUSIC algorithm when there are three TOA's.

first two dominant TOA's when there are actually ten TOA's. The dashed lines correspond to the case in which there are only two TOA's and we want to estimate these two TOA's.

In Figs. 15–18, we can see that the performance degrades a little when the number of TOA's is ten in comparison with the case that there are only two TOA's. Although there is some degradation in

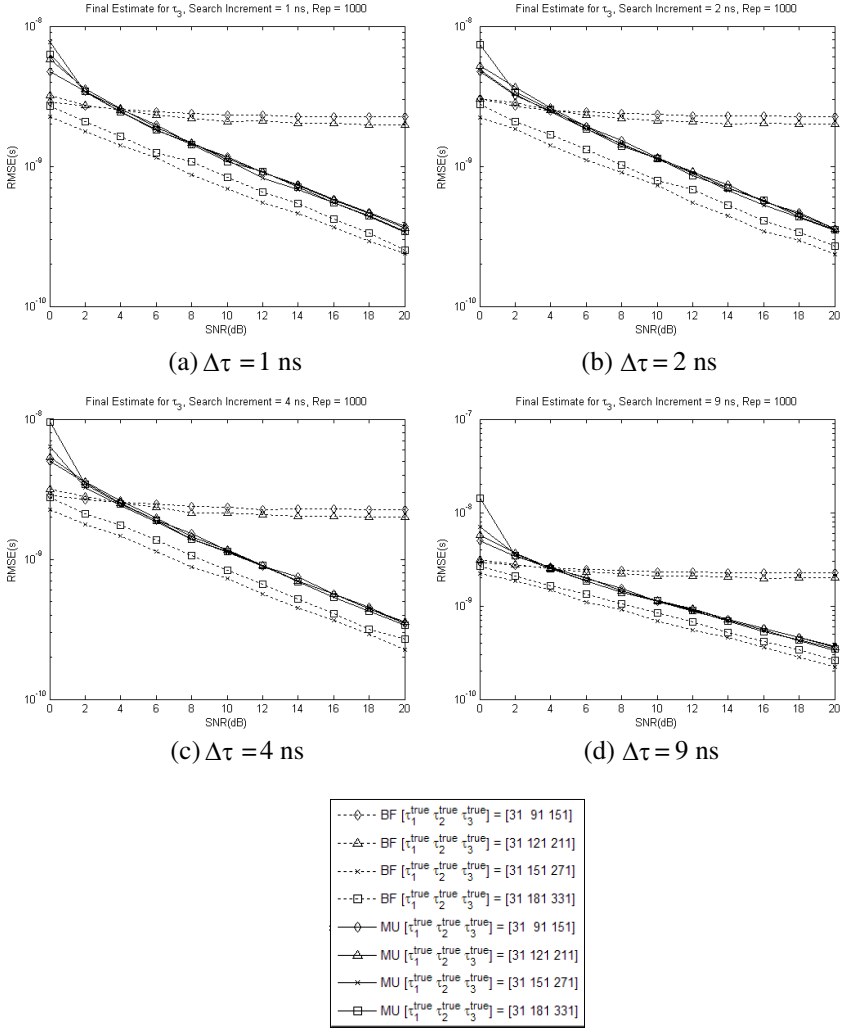

Figure 24. Final estimates of the third delay obtained from the beamforming algorithm and the MUSIC algorithm when there are three TOA's.

performance, it is easy to see that the proposed scheme still works when there are ten TOA's.

We considered the case that there are three TOA's. From Figs. 19–24, we compared the performance of the beamforming algorithm with that of the MUSIC algorithm. When the separation among the TOA's is small, the MUSIC algorithm outperforms the beamforming

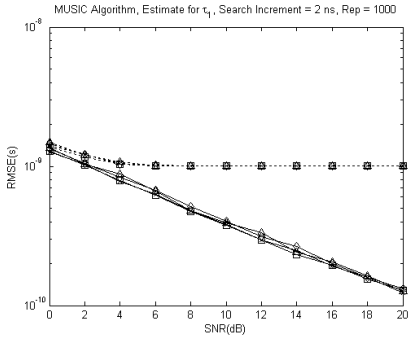

(a) $\Delta\tau = 2$ ns

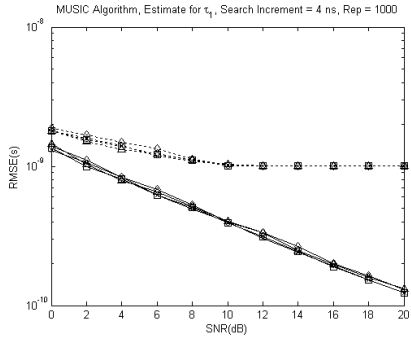

(b) $\Delta\tau = 4$ ns

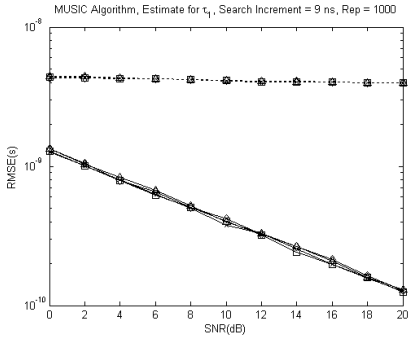

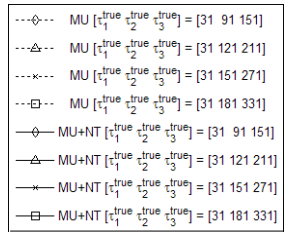

(c) $\Delta\tau = 9$ ns

Figure 25. Initial estimates and final estimates of the first delay obtained from the MUSIC algorithm when there are three TOA's.

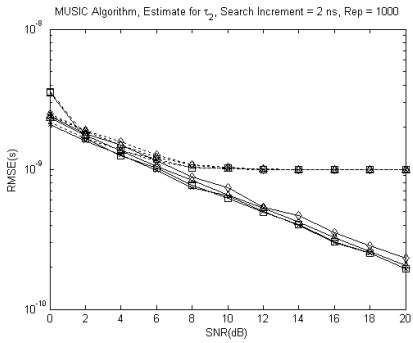

(a) $\Delta\tau = 2$ ns

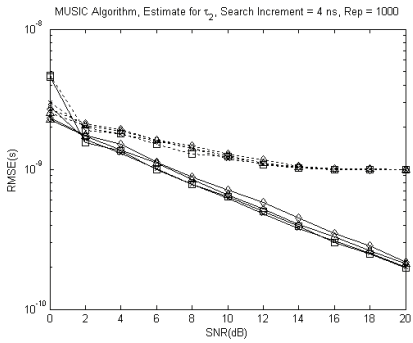

(b) $\Delta\tau = 4$ ns

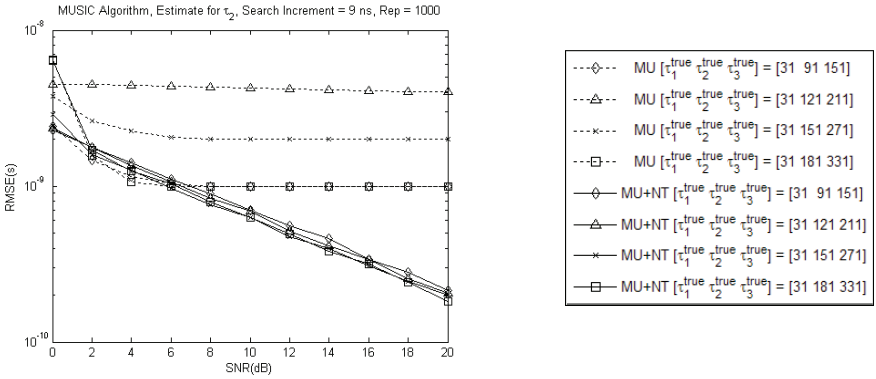

(c) $\Delta\tau = 9$ ns

Figure 26. Initial estimates and final estimates of the second delay obtained from the MUSIC algorithm when there are three TOA's.

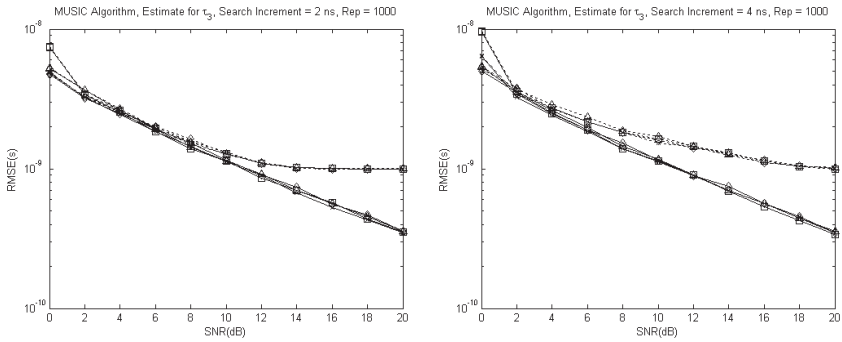

(a) $\Delta\tau = 2$ ns (b) $\Delta\tau = 4$ ns

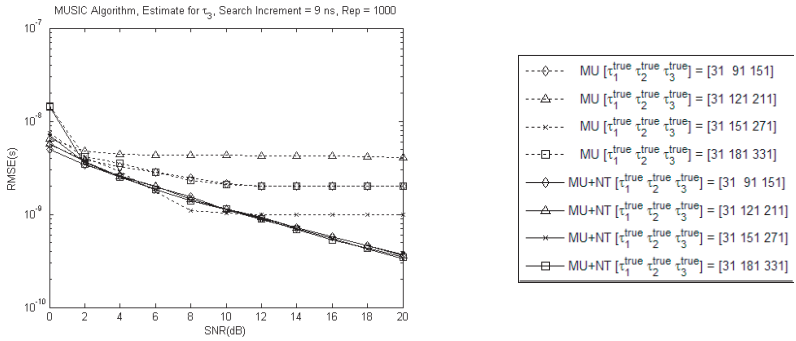

(c) $\Delta\tau = 9$ ns

Figure 27. Initial estimates and final estimates of the third delay obtained from the MUSIC algorithm when there are three TOA's.

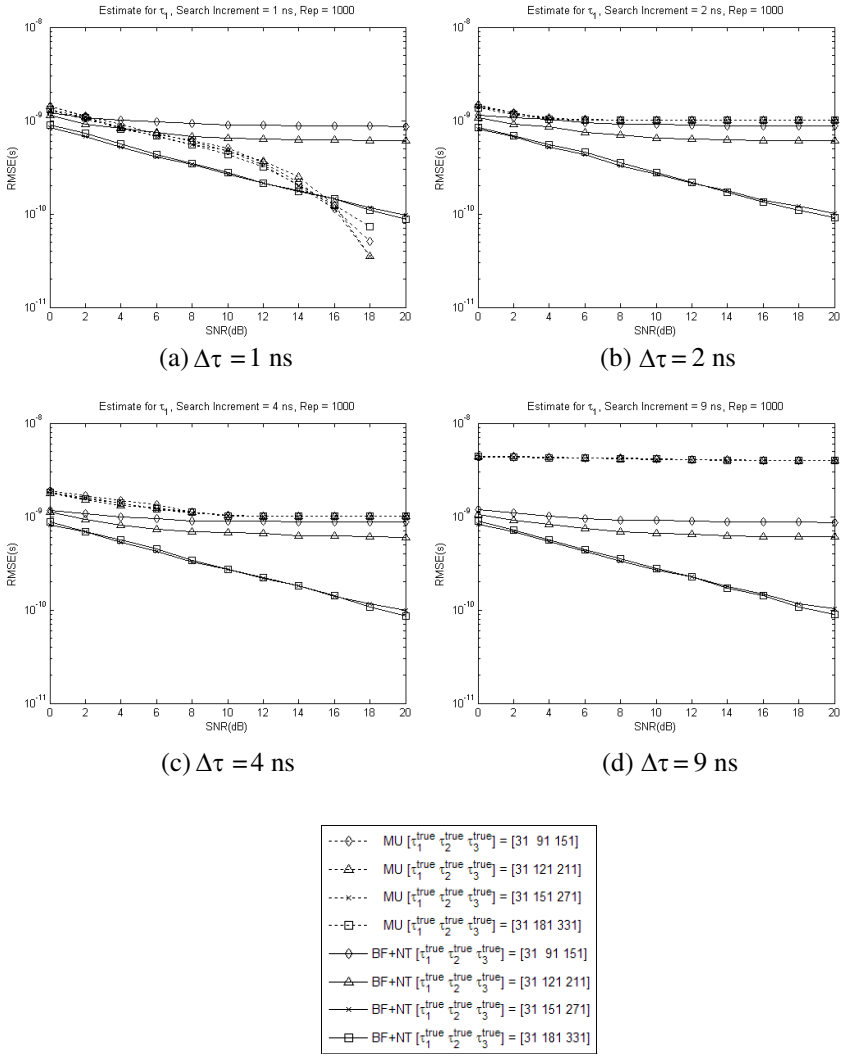

Figure 28. Initial estimates of the first delay obtained from the MUSIC algorithm and final estimates of the first delay obtained from the beamforming algorithm when there are three TOA's.

algorithm due to the superresolution property of the MUSIC algorithm. On the other hand, when the separation among TOA's is large, the beamforming algorithm outperforms the MUSIC algorithm. In the legend, 'BF' and 'MU' represent the results of the beamforming

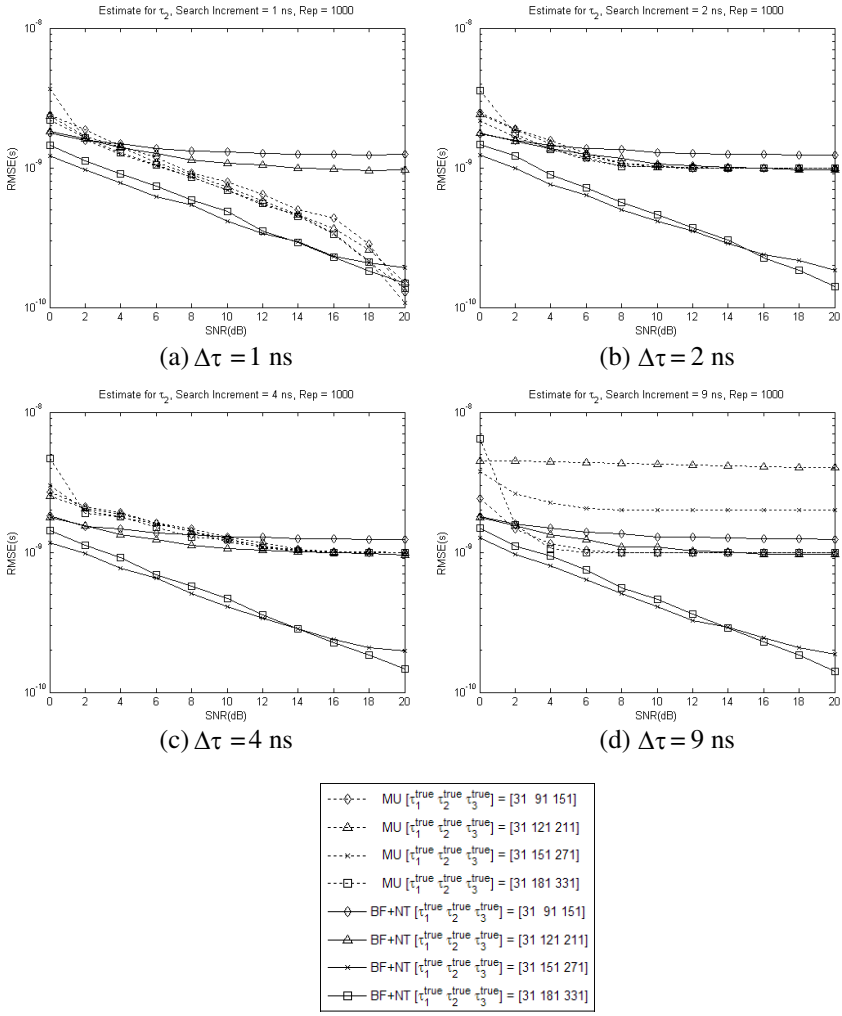

Figure 29. Initial estimates of the second delay obtained from the MUSIC algorithm and final estimates of the second delay obtained from the beamforming algorithm when there are three TOA's.

algorithm and the MUSIC algorithm, respectively.

In Figs. 25–27, we compared the accuracy of the initial estimates and the final estimates when there are three TOA's. In the legend, 'MU' and 'MU+NT' correspond to the initial estimate of the MUSIC algorithm and the final estimate of the MUSIC algorithm, respectively.

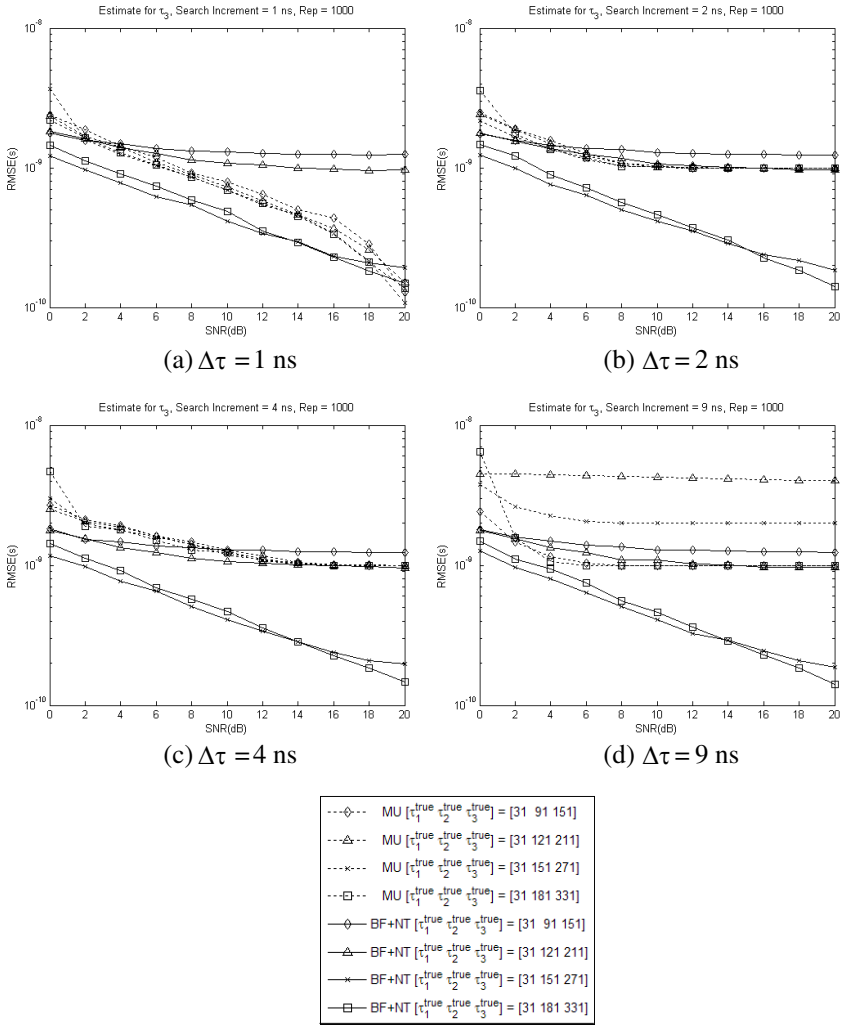

Figure 30. Initial estimates of the third delay obtained from the MUSIC algorithm and final estimates of the third delay obtained from the beamforming algorithm when there are three TOA's.

In Figs. 28–30, we compared the accuracy of the initial estimate of the MUSIC algorithm with that of the final estimate of the beamforming algorithm. In most cases, we can see that the final estimate of the beamforming algorithm is more accurate than the initial estimate of the MUSIC algorithm. In the legend, 'MU' and 'BF+NT'

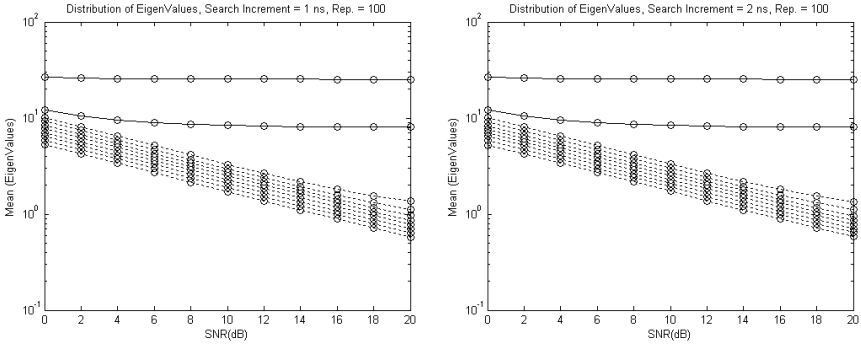

(a) $\Delta\tau = 1$ ns (b) $\Delta\tau = 2$ ns

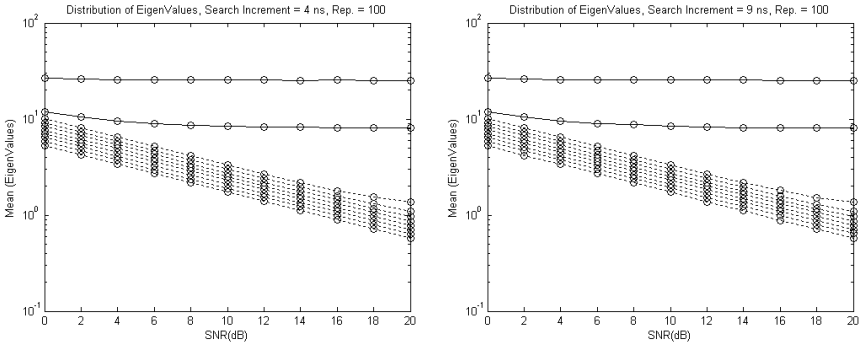

(c) $\Delta\tau = 4$ ns (d) $\Delta\tau = 9$ ns

Figure 31. Distribution of eigenvalues for $[\hat{\tau}_1^{(\text{true})} \quad \hat{\tau}_2^{(\text{true})}] = [31 \text{ ns } 91 \text{ ns}]$.

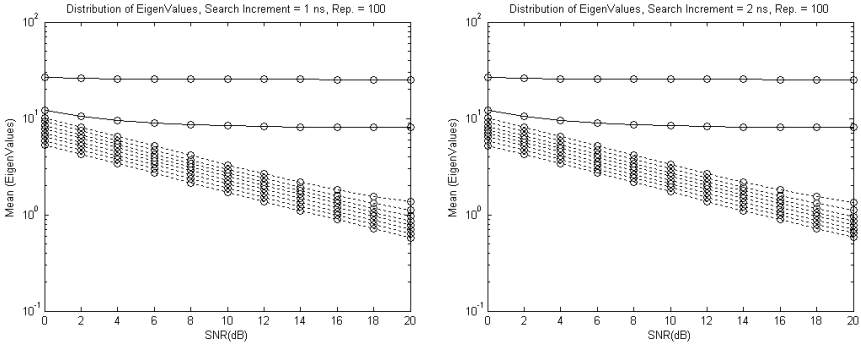

(a) $\Delta\tau = 1$ ns (b) $\Delta\tau = 2$ ns

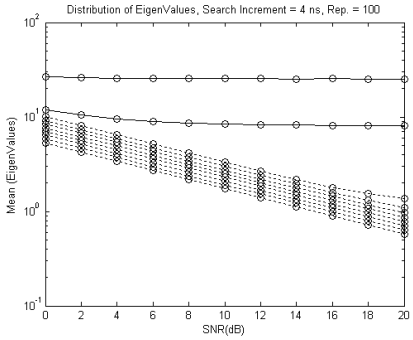

(c) $\Delta\tau = 4$ ns

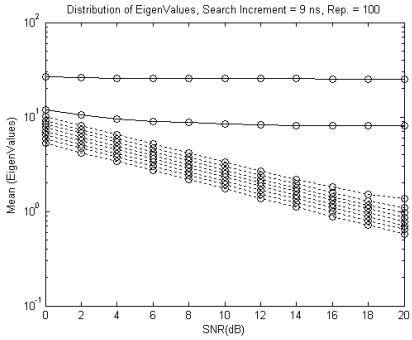

(d) $\Delta\tau = 9$ ns

Figure 32. Distribution of eigenvalues for $[\hat{\tau}_1^{(\text{true})} \quad \hat{\tau}_2^{(\text{true})}] = [31 \text{ ns } 121 \text{ ns}]$.

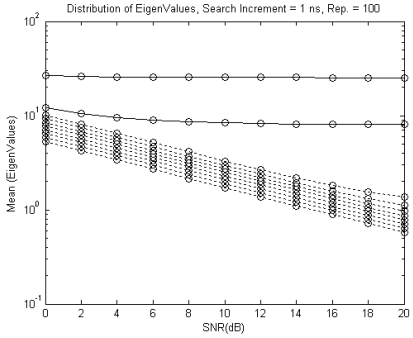

(a) $\Delta\tau = 1$ ns

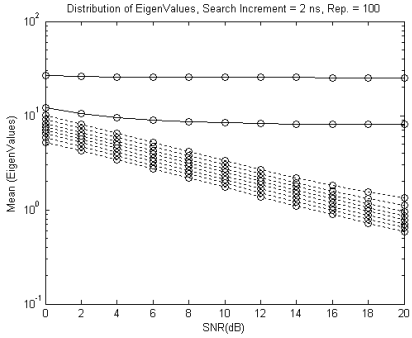

(b) $\Delta\tau = 2$ ns

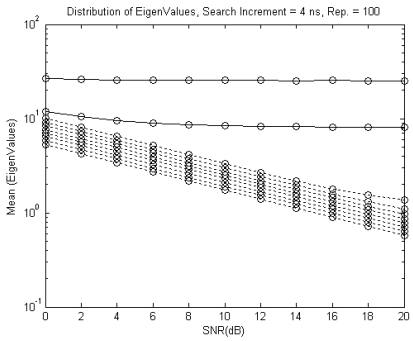

(c) $\Delta\tau = 4$ ns

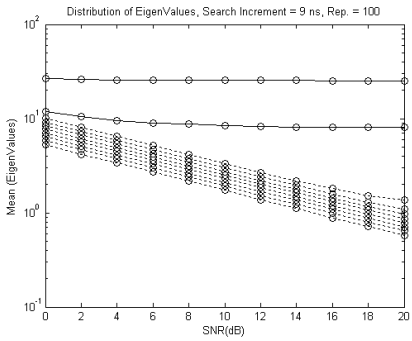

(d) $\Delta\tau = 9$ ns

Figure 33. Distribution of eigenvalues for $[\hat{\tau}_1^{(\text{true})} \quad \hat{\tau}_2^{(\text{true})}] = [31 \text{ ns } 151 \text{ ns}]$.

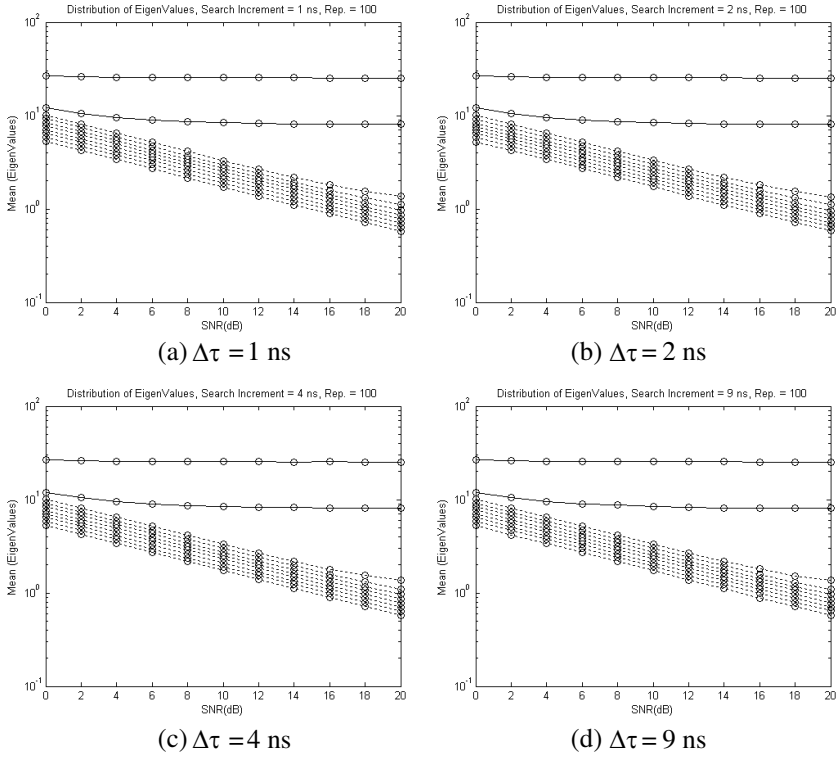

(a) $\Delta\tau = 1$ ns (b) $\Delta\tau = 2$ ns

(c) $\Delta\tau = 4$ ns (d) $\Delta\tau = 9$ ns

Figure 34. Distribution of eigenvalues for $[\hat{\tau}_1^{(\text{true})} \quad \hat{\tau}_2^{(\text{true})}] = [31 \text{ ns } 181 \text{ ns}]$.

correspond to the initial estimate of the MUSIC algorithm and the final estimate of the beamforming algorithm, respectively.

In the case that the number of parameters is not known a priori, we can estimate the number of parameters from the effective rank of the covariance matrix in (9).

In Figs. 31–34, we have shown the distribution of the eigenvalues to see whether it's possible to estimate the effective number of the parameters from the distribution of the eigenvalues. The average values of 100 repetitions are shown. When SNR is higher than or equal to SNR = 2 dB, it is quite easy to recognize that the number of TOA's to be estimated is two from the distribution of the eigenvalues. Note that the number of TOA parameters to be estimated is equal to the effective rank of the covariance matrix.

5. CONCLUSION

In this paper, we propose that the Newton iteration can be applied to the TOA estimation to improve the accuracy of the initial estimate for the beamforming algorithm and the MUSIC algorithm. We apply the Newton iteration to the initial estimate obtained from the beamforming algorithm and the MUSIC algorithm to obtain the final estimate which is more accurate than the initial estimate. We have demonstrated the performance improvement using the various numerical results. Besides the beamforming algorithms and the MUSIC algorithm, it is quite straightforward to get the suggested scheme applied to the any other TOA estimation algorithms.

ACKNOWLEDGMENT

This work was supported by the National Research Foundation of Korea Grant funded by the Korean Government (NRF-2010-013-D00045).

This research was supported by Basic Science Research Program through the National Research Foundation of Korea (NRF) funded by the Ministry of Education, Science and Technology (2010-0011042).

REFERENCES

1. Jeong, Y.-S. and J.-H. Lee, "Estimation of time delay using conventional beamforming-based algorithm for UWB systems," *Journal of Electromagnetic Waves and Applications*, Vol. 21, No. 15, 2413–2320, 2007.
2. Yamada, H., M. Ohmiya, Y. Ogawa, and, K. Itoh, "Superresolution techniques for time-domain measurements with a network analyzer," *IEEE Trans. Antennas and Propagation*, Vol. 39, No. 2, 177–183, 1991.
3. Ki, X. and K. Pahlavan, "Super-resolution TOA estimation with diversity for indoor geolocation," *IEEE Trans. Wireless Communications*, Vol. 3, No. 1, 224–234, 2004.
4. Kwon, H.-J., J.-H. Lee, Y.-S. Jeong, and S.-H. Jo, "Timing synchronization for performance improvement of TOA in UWB MB-OFDM systems," *The Journal of Korea Information and Communications Society*, Vol. 32, No. 5, 550–555, May 2007.
5. Zhao, F., W. Yao, C. C. Logothetis, and Y. Song, "Super-resolution TOA estimation in OFDM systems for indoor

environments," *Proceedings of the IEEE International Conference on Networking, Sensing and Control*, 723–728, 2007.

6. Li, X., K. Pahlavan, and J. Beneat, "Performance of TOA estimation techniques in indoor multipath channels," *Proceedings of the 13th IEEE International Symposium on Personal, Indoor and Mobile Radio Communications*, Vol. 2, 911–915, 2002.
7. Sieskul, B. T., F. Zheng, and T. Kaiser, "A hybrid SS-ToA wireless NLoS geolocation based on path attenuation: ToA estimation and CRB for mobile position estimation," *IEEE Transactions on Vehicular Technology*, Vol. 58, No. 9, 4930–4942, 2009.
8. Wang, Y., G. Leus, and H. Delic, "TOA estimation using UWB with low sampling rate and clock drift calibration," *IEEE International Conference on Ultrawideband*, 612–617, 2009.
9. Zhang, T., Q. Zhang, and N. Zhang, "A two-step TOA estimation method based on energy detection for IR-UWB sensor networks," *Proceedings of Communication Networks and Services Research Conference (CNSR), Seventh Annual,* 139–145, 2009.
10. Kelley, C. T., *Solving Nonlinear Equations with Newton's Method*, No. 1 in Fundamentals of Algorithms, SIAM, 2003.
11. Ortega, J. M. and W. C. Rheinboldt, *Iterative Solution of Nonlinear Equations in Several Variables, Classics in Applied Mathematics*, SIAM, 2000.
12. Press, W. H., B. P. Flannery, S. A. Teukolsky, and W. T. Vetterling, "Numerical recipes: The art of scientific computing," Cambridge University Press, 2007, ISBN 0-521-88068-8 (available for a fee online, with code samples [4]).
13. Tayebi, A., J. Gomez, F. Saez de Adana, and O. Gutierrez, "The application of ray-tracing to mobile localization using the direction of arrival and received signal strength in multipath indoor environments," *Progress In Electromagnetics Research*, Vol. 91, 1–15, 2009.
14. Chen, J.-F., Z.-G. Shi, S.-H. Hong, and K. S. Chen, "Grey prediction based particle filter for maneuvering target tracking," *Progress In Electromagnetics Research*, Vol. 93, 237–254, 2009.
15. Song, H. B., H.-G. Wang, K. Hong, and L. Wang, "A novel source localization scheme based on unitary esprit and city electronic maps in urban environments," *Progress In Electromagnetics Research*, Vol. 94, 243–262, 2009.
16. Liu, H.-Q., H.-C. So, K. W. K. Lui, and F. K. W. Chan, "Sensor selection for target tracking in sensor networks," *Progress In Electromagnetics Research*, Vol. 95, 267–282, 2009.

17. Liu, H.-Q. and H.-C. So, "Target tracking with line-of-sight identification in sensor networks under unknown measurement noises," *Progress In Electromagnetics Research*, Vol. 97, 373–389, 2009.
18. Lazaro, A., D. Girbau, and R. Villarino, "Wavelet-based breast tumor localization technique using a UWB radar," *Progress In Electromagnetics Research*, Vol. 98, 75–95, 2009.
19. Mitilineos, S. A. and S. C. A. Thomopoulos, "Positioning accuracy enhancement using error modeling via a polynomial approximation approach," *Progress In Electromagnetics Research*, Vol. 102, 49–64, 2010.
20. Zhang, W., A. Hoorfar, and L. Li, "Through-the-wall target localization with time reversal MUSIC method," *Progress In Electromagnetics Research*, Vol. 106, 75–89, 2010.
21. Mitilineos, S. A., D. M. Kyriazanos, O. E. Segou, J. N. Goufas, and S. C. A. Thomopoulos, "Indoor localisation with wireless sensor networks," *Progress In Electromagnetics Research*, Vol. 109, 441–474, 2010.
22. Bahillo Martinez, A., S. Mazuelas Franco, J. Prieto Tejedor, R. M. Lorenzo Toledo, P. Fernandez Reguero, and E. J. Abril, "Indoor location based on IEEE 802.11 round-trip time measurements with two-step NLOS mitigation," *Progress In Electromagnetics Research B*, Vol. 15, 285–306, 2009.
23. Lazaro, A., D. Girbau, and R. Villarino, "Weighted centroid method for breast tumor localization using an UWB radar," *Progress In Electromagnetics Research B*, Vol. 24, 1–15, 2010.
24. Gomez, J., A. Tayebi, F. Saez de Adana, and O. Gutierrez, "Localization approach based on ray-tracing including the effect of human shadowing," *Progress In Electromagnetics Research Letters*, Vol. 15, 1–11, 2010.
25. Liang, G., W. Gong, H. Liu, and J. Yu, "Development of 61-channel digital beamforming (DBF) transmitter array for mobile satellite communication," *Progress In Electromagnetics Research*, Vol. 97, 177–195, 2009.
26. Liang, G., W. Gong, H. Liu, and J. Yu, "A semi-physical simulation system for DBF transmitter array on Leo satellite," *Progress In Electromagnetics Research*, Vol. 97, 197–215, 2009.
27. Li, G., S. Yang, Y. Chen, and Z.-P. Nie, "A novel electronic beam steering technique in time modulated antenna array," *Progress In Electromagnetics Research*, Vol. 97, 391–405, 2009.
28. O'Halloran, M., M. Glavin, and E. Jones, "Channel-ranked

beamformer for the early detection of breast cancer," *Progress In Electromagnetics Research*, Vol. 103, 153–168, 2010.

29. Yang, P., F. Yang, and Z.-P. Nie, "DOA estimation with subarray divided technique and interporlated ESPRIT algorithm on a cylindrical conformal array antenna," *Progress In Electromagnetics Research*, Vol. 103, 201–216, 2010.
30. Alsehaili, M., S. Noghanian, A. R. Sebak, and D. A. Buchanan, "Angle and time of arrival statistics of a three dimensional geometrical scattering channel model for indoor and outdoor propagation environments," *Progress In Electromagnetics Research*, Vol. 109, 191–209, 2010.
31. Castaldi, G., V. Galdi, and G. Gerini, "Evaluation of a neural-network-based adaptive beamforming scheme with magnitude-only constraints," *Progress In Electromagnetics Research B*, Vol. 11, 1–14, 2009.
32. Palanisamy, P. and N. Rao, "Direction of arrival estimation based on fourth-order cumulant using propagator method," *Progress In Electromagnetics Research B*, Vol. 18, 83–99, 2009.
33. Zhang, X., G. Feng, and D. Xu, "Blind direction of angle and time delay estimation algorithm for uniform linear array employing multi-invariance MUSIC," *Progress In Electromagnetics Research Letters*, Vol. 13, 11–20, 2010.